Biochemical Pharmacology 102 (2016) 78–96

Contents lists available at ScienceDirect

Biochemical Pharmacology

journal homepage: www.elsevier.com/locate/biochempharm

Pharmacological inhibition of eicosanoids and platelet-activating factor signaling impairs zymosan-induced release of IL-23 by dendritic cells

Mario Rodríguez[a], Saioa Márquez[a], Olimpio Montero[b], Sara Alonso[c], Javier García Frade[d], Mariano Sánchez Crespo[c,*], Nieves Fernández[a]

[a] Departamento de Bioquímica y Biología Molecular, Facultad de Medicina, Universidad de Valladolid, 47005 Valladolid, Spain
[b] Centro para el Desarrollo de la Biotecnología, CSIC, Parque Tecnológico de Boecillo, Valladolid, Spain
[c] Instituto de Biología y Genética Molecular, CSIC, 47003 Valladolid, Spain
[d] Servicio de Hematología, Hospital Universitario Rio-Hortega, 47012 Valladolid, Spain

ARTICLE INFO

Article history:
Received 23 September 2015
Accepted 2 December 2015
Available online 7 December 2015

Chemical compounds studied in this article:
Acetyl-CoA (PubChem CID: 444493)
Arachidonoyl-CoA (PubChem CID: 52922027)
Darapladib (PubChem CID: 9939609)
EDC (2-TEDC, PubChem CID: 6069552)
12-HETE (PubChem CID: 5353272)
12-HETE-d8 (PubChem CID: 1436)
Leukotriene B_4 (PubChem CID: 5280492)
Leukotriene B_4-d4 (PubChem CID: 53394387)
Leukotriene C_4 (PubChem CID: 5280493)
Leukotriene E_4 (PubChem CID: 5280879)
Lyso-PAF C16:0 (PubChem CID: 3983)
Montelukast (PubChem CID: 5281040)
PGE_2 (PubChem CID: 5280360)
Platelet-activating factor (PubChem CID: 108156)
PAF C16:0-d4 (PubChem CID: 53394395)
PAF C18:0 (PubChem CID: 2733535)
U75302 (PubChem CID: 6449854)
WEB2086 (Apafant, PubChem CID: 65889)

Keywords:
Cytokines
Dendritic cells
Fungus
Lipid mediators
Signal transduction

ABSTRACT

The engagement of the receptors for fungal patterns induces the expression of cytokines, the release of arachidonic acid, and the production of PGE_2 in human dendritic cells (DC), but few data are available about other lipid mediators that may modulate DC function. The combined antagonism of leukotriene (LT) B_4, cysteinyl-LT, and platelet-activating factor (PAF, 1-*O*-alkyl-2-acetyl-*sn*-glycero-3-phosphocholine) inhibited *IL23A* mRNA expression in response to the fungal surrogate zymosan and to a lower extent *TNFA* (tumor necrosis factor-α) and *CSF2* (granulocyte macrophage colony-stimulating factor) mRNA. The combination of lipid mediators and the lipid extract of zymosan-conditioned medium increased the induction of *IL23A* by LPS (bacterial lipopolysaccharide), thus suggesting that unlike LPS, zymosan elicits the production of mediators at a concentration enough for optimal response. Zymosan induced the release of LTB_4, LTE_4, 12-hydroxyeicosatetraenoic acid (12-HETE), and PAF C16:0. DC showed a high expression and detectable Ser663 phosphorylation of 5-lipoxygenase in response to zymosan, and a high expression and activity of LPCAT1/2 (lysophosphatidylcholine acyltransferase 1 and 2), the enzymes that incorporate acetate from acetyl-CoA into choline-containing lysophospholipids to produce PAF. Pharmacological modulation of the arachidonic acid cascade and the PAF receptor inhibited the binding of P-71Thr-ATF2 (activating transcription factor 2) to the *IL23A* promoter, thus mirroring their effects on the expression of *IL23A* mRNA and IL-23 protein. These results indicate that LTB_4, cysteinyl-LT, and PAF, acting through their cognate G protein-coupled receptors, contribute to the phosphorylation of ATF2 and play a central role in *IL23A* promoter *trans*-activation and the cytokine signature induced by fungal patterns.

* Corresponding author at: Instituto de Biología y Genética Molecular, C/Sanz y Forés 3, 47003 Valladolid, Spain. Fax: +34 983 184800.
E-mail address: mscres@ibgm.uva.es (M.S. Crespo).

http://dx.doi.org/10.1016/j.bcp.2015.12.001
0006-2952/

1. Introduction

The cytokines of the IL-12 family IL-12 p70 and IL-23 polarize the immune response into the Th1 and Th17 types, respectively. These cytokines share a common chain, IL-12 p40, encoded by the gene *IL12B*, and differ in a specific chain for each cytokine, IL-12 p35 (gene *IL12A*) for IL-12 p70, and IL-23 p19 (gene *IL23A*) for IL-23. A corollary to this structural feature is that the regulation of the expression of these chains is critical to the polarization of the immune response during fungal invasion. The fungal surrogate zymosan, which is mainly composed of β-glucans and α-mannans, stands out as a strong stimulus for IL-23 production, whereas it inhibits the expression of IL-12 p70 through the transcriptional repression of *IL12A* [1–4]. These findings are of pathophysiological relevance because the recognition of β-glucans and α-mannans is a central component of the host defense during the infection by microbes such as *Candida*, *Aspergillus*, and *Pneumocystis jirovecii*. In addition to the relevance of these facts to the pathophysiology of infectious diseases, the mechanistic data regarding IL-23 regulation are of major importance to understand the pathogenesis of autoimmune and autoinflammatory diseases such as ankylosing spondylitis, psoriasis, intestinal bowel disease, and multiple sclerosis. Recent studies on the transcriptional regulation of *IL23A* extended previous research on the role of ATF2 (activating transcription factor 2) [5,6] by disclosing its dependence on the complementary phosphorylations of its Thr69 and Thr71 [7]. Enhancement of IL-23 production in the LPS/TLR4 route by PGE_2 has been reported [8–11], but these studies have unveiled different results depending on the cell type and an opposing effect of PGE_2 receptor-dependent signals on the expression of either IL-12 p40 or IL-23 p19 chains. Whereas there is a consensus regarding the down-regulatory effect of E prostanoid receptors (EP) on the transcriptional activity of *IL12B*, *IL23A* transcription is activated by EP signaling, in particular following EP4 engagement [10]. However, the overall role of the lipid mediator cascade in the polarization of the cytokine response has not been assessed and this is a critical factor in the response to fungal patterns, because both zymosan and *Candida* are archetypal stimuli that trigger the generation of eicosanoids in the innate immune system [12–15]. The *Candida* paradigm posits that β-glucans and α-mannans engage C-type lectin receptors in macrophages and dendritic cells and activate a signaling cascade that promotes the phosphorylation- and Ca^{2+}-dependent activation of the cytosolic phospholipase $A_2\alpha$ ($cPLA_2$), thus leading to an early production of eicosanoids that influence gene expression [16]. In contrast, LPS elicits delayed onset changes of the eicosanome related to the induction of enzymes of the cyclooxygenase route [17]. In this study, we have assayed the lipid mediators produced by zymosan in human monocyte-derived dendritic cells (DC) and their role on the modulation of the expression of *IL23A*. Our results have shown a strong induction of arachidonic acid (AA) release and its partial conversion into a wide set of oxidation products, which include prostaglandin (PG) E_2, 12-hydroxyeicosatetraenoic acid (12-HETE), leukotriene (LT) B_4, and LTE_4; as well as the biosynthesis of the phospholipid mediator 1-hexadecyl-2-acetyl-*sn*-glycero-3-phosphocholine (platelet-activating factor, PAF). The combined action of LTB_4, cysteinyl-LT, and PAF on their G protein-coupled receptors elicits strong signals leading to the phosphorylation of ATF2 that explain its activation and its ensuing effect on *IL23A* promoter *trans*-activation. This study contributes to ascertain the role of lipid mediators in the induction of the cytokine signature elicited by fungal patterns by disclosing the role of the products generated upon the activation of $cPLA_2$ and the ensuing acetylation of 1-hexadecyl-2-lyso-glycero-3-phosphocholine by lysophosphatidylcholine acyltransferases (LPCAT) on the regulation of *IL23A*.

2. Materials and methods

2.1. Cells and reagents

DC were obtained from human mononuclear cells collected from pooled buffy coats of healthy donors provided by Centro de Hemoterapia de Castilla y León. The differentiation of monocytes was carried out by culture in the presence of GM-CSF and IL-4 for 5 days and assessed by flow cytometry of CD40, CD80, CD83, and CD86 as previously reported [13]. Zymosan from *Saccharomyces cerevisiae*, mannan, the 5-lipoxygenase (5-LO) inhibitor zileuton, the PAF-receptor antagonist WEB2086, acetyl-CoA, lyso-PAF C16:0, and LPS were from Sigma Chemical Co. (St. Louis, MO). The pyrrolidine-1 derived $cPLA_2$ inhibitor (Cat. No. 525143) was from Calbiochem-Merck Millipore (Billerica, MA). The 12/15-LO inhibitor ethyl 3,4-dihydroxybenzylidenecyanoacetate (EDC) and AA-CoA lithium salt were from Santa Cruz Biotechnology (Dallas, TX). The PAF-acetylhydrolase (also known as lipoprotein-associated phospholipase A_2) inhibitor darapladib was from Selleckchem (Houston, TX). The cysteinyl-LT receptor 1 (CysLT1) antagonist montelukast, the LTB_4 receptor 1 (BLT1) antagonist U75302, specific ELISA assays for LTB_4 and E_4, and deuterated standards for MS were from Cayman Chemical (Ann Arbor, MI). These ELISA assays were carried out following the manufacturer's protocol in lipid extracts obtained using Strata™ C-18E SPE cartridges (Phenomenex Inc. Torrance, CA). Reagents for the ELISA assay of IL-23 in the DC supernatants were from R&D Systems (Minneapolis, MN).

2.2. Ethics statement

The study was approved by the Bioethical Committee of the Spanish Council of Research (CSIC) before starting the study and the written informed consent of all healthy donor subjects was obtained at Centro de Hemoterapia y Hemodonación de Castilla y León Biobank. The participants received written consent according to the regulations of the Biobank. The researchers received the samples in an anonymous way. The experiments conformed to the principles set out in the WMA Declaration of Helsinki. The process is documented by the Biobank authority according to the specific Spanish regulations.

2.3. Real-time RT-PCR

Total RNA was obtained by TRIzol/chloroform extraction and used for RT reactions. The resulting cDNA was amplified in a PTC-200 apparatus equipped with a Chromo4 detector (Bio-Rad) using SYBR Green I mix containing Hot Start polymerase (ABgene). Cycling conditions were consistent with the melting temperatures of each set of primers. *GAPDH* was used as a housekeeping gene to assess the relative abundance of the different mRNA, using the comparative cycle threshold method. The procedure was used to assay *IL23A*, *IL12B*, *IL10*, *TNFA*, *CSF2*, *LPCAT*, *LPCAT2*, *LPCAT3*, *ALOX12*, *ALOX15*, *PTAFR*, and *GADPH* mRNA. The sequences of the primers and the reaction conditions are shown in Table 1.

2.4. Chromatin immunoprecipitation (ChIP) assay

ChIP assays were conducted with 10 μg of Ab against P-ATF2 (Thr71, Cell Signaling # 9221), anti-P-CREB (Ser133, Millipore # 06-519), and irrelevant Ab as previously reported [18]. Briefly, cells were stimulated and then washed twice with PBS and fixed with 1% formaldehyde. Cross-linking was terminated by 0.125 M glycine.

Table 1
Primers used for ChIP and RT-PCR reactions.

Promoter primers	Melting temperatures (°C)
IL23A CRE S: 5′-AGACCTCCATTCAGGACAAG-3′	57.3
IL23A CRE AS: 5′-TCGAAGACGTCAGAATGAGG-3′	57.3
IL23A ATF2 S: 5′-CATTGCAAACAGCTCACCAT-3′	58.2
IL23A ATF2 AS: 5′-ATTTCCTCACTTCCTCCTGC-3′	56.9
IL12A control S: 5′-GCGAACATTTCGCTTTCATT-3′	58.8
IL12A control AS: 5′-ACTTTCCCGGGACTCTGGT-3′	59.4
Coding sequence primers	**Melting temperatures (°C)**
IL23A S: 5′-CATGGGCCTTCATGCTATTT-3′	58.4
IL23A AS: 5′-TTT GCATTG TCAGGTTTCCA-3′	58.5
IL12B S: 5‘-CATGGGCCTTCATGCTATTT-3‘	55.3
IL12B AS: 5‘-TTTGCATTGTCAGGTTTCCA-3‘	53.2
IL10 S: 5′-GAGAACAGCTGCACC CAC TT-3′	59.4
IL10 AS: 5′-GGCCTTGCTCTTGTT TTC AC-3′	57.3
CSF2 S: 5′-GGCTAAAGTTCTCTGGAGGAT-3′	57.9
CSF2 AS: 5′-ACTGTTTCATTCATCTCAGCAG-3′	56.5
TNFA S: 5′-GTTGTAGCAAACCCTCAA-3′	57.3
TNFA AS: 5′-TTGAAGAGGACCTGGGA-3′	57.3
LPCAT1 S: 5′-GCTGGCTTTCAAGATGTACG-3′	57.3
LPCAT1 AS: 5′-TCAATGGCTCGGAATAGGTC-3′	55.3
LPCAT2 S: 5′-TTGCTTCCAATTCGTGTCTTATT-3′	57.3
LPCAT2 AS: 5′-ATCCCATTGAAAAGAACATAGCA-3′	55.3
LPCAT3 S: 5′-CAGGGAGAGCTGATTGACAT-3′	57.3
LPCAT3 AS: 5′-CAGAAGGGGTGGTTGTCATA-3′	57.3
ALOX12 S: 5′-CACCATGGAAATCAACACCC-3′	55.3
ALOX12 AS: 5′-GTGCTCACTGCCTTATCAAA-3′	58.8
ALOX15 S: 5′-CTTGCTCTGACCACACCAGA-3′	59.4
ALOX15 AS: 5′-GCTGGGGCCAAACTATATGA-3′	57.3
PTAFR S: 5′-CTGCTGTTTCTCAGGCA-3′ transcript variant 2	56
PTAFR S: 5′-CAGACAGAGACACACGGTC-3′ transcript variants 1, 3, and 4	58.8
PTAFR AS: 5′-GAACTCAGAGTCCATGTGGG-3′ transcript variants 1–4	59.4
GAPDH S: 5′-GTCAGTGGTGGACCTGACCT-3′	61.4
GAPDH AS: 5′-AGGGGAGATTCAGTGTGGTG-3′	59.4

The PCR conditions were adapted to each primer sets, but in most cases were 5 min at 95 °C (hot start), 45 cycles of denaturation at 95 °C for 15 s, annealing at 60 °C for 20 s, and elongation at 72 °C, 1 min/kb. Final extension was carried out at 72 °C for 5 min.
Melting temperatures are indicated to show the adequacy of the reaction conditions for each set of primers.

Crude nuclear extracts were collected by microcentrifugation and resuspended in a lysis buffer containing a high salt concentration. Chromatin sonication was carried out using a Bioruptor device from Diagenode (Liege, Belgium). The chromatin solution was precleared by adding Protein A/G PLUS-Agarose for 30 min at 4 °C under continuous rotation. After elimination of the beads, Ab was added for overnight incubation at 4 °C, and then Protein A/G PLUS-Agarose was added and incubated for an additional period of 2 h at 4 °C. Beads were harvested by centrifugation at 4000 × *g* and sequentially washed with lysis buffer high salt, wash buffer, and elution buffer. Cross-links were reversed by heating at 67 °C in a water bath and the DNA bound to the beads isolated by extraction with phenol/chloroform/isoamylalcohol. Irrelevant Ab and sequences of the *IL12A* promoter were used as a control of binding specificity. The promoter primer sequences are shown in Table 1.

2.5. Assay of lipid mediators by reversed phase UPLC and electrospray ionization quadrupole time-of-flight MS

Initial studies were conducted in the medium used for cytokine induction to mimic most exactly the experimental conditions of the assays. Accordingly, FBS was not removed from the medium. Since the results suggested that the presence of FBS may affect the processing of both LT and PAF due to both the presence of inactivating enzymes and lipids in FBS, additional experiments were carried out using serum-free DMEM supplemented with 0.25% delipidated BSA or 0.1% standard BSA. Deuterated standards were added after collecting the samples. Lipids were extracted into ethanol from cell supernatants (15% final), eluted in methanol using Strata™ C-18E SPE cartridges, and evaporated to dryness under N_2. The lipid residue was solubilized in 40 μl UPLC solvent A (8.3 mM acetic acid buffered to pH 5.7 with ammonium hydroxide) plus 20 μl UPLC solvent B (acetonitrile/methanol 65:35, v/v). Two different gradients were used to improve compound detection. A 7.5 μl aliquot of each sample was injected into the chromatographic system. The chromatographic separation was conducted in an Acquity™ UPLC System (Waters, Manchester, UK) equipped with an Acquity UPLC® BEH C18, 1.7 μm, 2.1 × 100 mm column (Waters). The chromatographic column was directly interfaced into the electrospray ionization source of a mass spectrometer (SYNAPT HDMS G2, Waters). MS analysis was performed in negative ion mode using a MS^E method that allows simultaneous detection of analytes through a low energy function (full scan) and a high energy function (collision energy) with ion partial fragmentation. The mass spectrometer was operated in sensitivity mode with 5 ppm threshold for maximum RMS residual mass. Sodium formate was used for calibration and leucine-enkephalin (*m*/*z* 554.2615) for reference of mass accuracy. For quantification, external standards of PGE_2, PGD_2, LTB_4, 12-HETE, 15-HETE, PAF C16:0, PAF C18:0, and AA were used to draw a linear regression of chromatographic peak area to compound concentration. All compounds were identified by injecting authentic standards and by exact mass along with fragmentation pattern as observed in the high energy function. The parent ions of *m*/*z* 351.217, *m*/*z* 335.222, *m*/*z* 319.22, and *m*/*z* 303.233 as obtained in the low energy function, were used for quantification of PGE_2, LTB_4, 12-HETE, and

AA, respectively, while the fragment ion of *m/z* 315.196 was used for quantification of PGD_2. For PAF assay, Bligh and Dyer extraction was used and chromatography was carried out at a flow rate of 0.35 ml/min using the gradient that follows: initial, 100% A; 1 min, 100% A; 2.5 min, 20% A; 4 min, 20% A; 5.5 min, 0.1% A; 8.0 min, 0.1% A; 10 min, 100% A, and this was kept isocratic for 2 min to recover initial pressure before next injection. Solvents were (A) methanol/water/formic acid (50:50:0.5, v/v/v) and (B) methanol/acetonitrile/formic acid (59:40:0.5, v/v/v), both with 5 mM ammonium formate. An extract volume of 7.5 ml was injected. Mass spectrometer parameters were fitted as follows: capillary, 0.9 kV; sampling cone, 18 V; source temperature, 90 °C; desolvation temperature, 320 °C; cone gas, 45 l/h; and desolvation gas, 900 l/h. Data were acquired with the software MassLynx at a rate of 5 scans/s within the range 0–12 min and 100–1200 Da *m/z* for the low-energy function, and 50–900 Da *m/z* for the high-energy function (MS^E method, trap collision energy 30 V), with ionization in positive mode (ESI+). PAF was detected and quantified as the $[M+H]^+$ ion *m/z* 524.3711 and *m/z* 552.4024 for PAF C16:0 and PAF C18:0, respectively.

2.6. Laser-scanning confocal fluorescence microscopy

DC were seeded on polylysine-coated glass coverslips for 12 h and then stimulated with zymosan particles. Cells were fixed with 10% formaldehyde in PBS and stained with anti-5-LO Ab (0.3 μg in 30 μl per coverslip) (Cell Signaling # 3289) and goat anti-rabbit IgG Ab labelled with Alexa-Fluor®480 (1:100 v/v). In both cases the incubation times were 1 h at room temperature in the dark. The coverslips were observed by laser-scanning confocal fluorescence microscopy using a Leica TCS SP5 apparatus (Leica Microsystems CMS GmbH, Mannheim, Germany) equipped with a white-light laser and a Leica 63PL APO NA 1.40 oil immersion objective. Image analysis and subcellular colocalization fluorograms were generated and analyzed using a Leica confocal software package and Adobe Photoshop CS5.1 software (Adobe Systems, San Jose, CA).

2.7. Immunoprecipitation of 5-LO

DC were lysed in a medium containing 20 mM Tris–HCl, 150 mM NaCl, 5 mM EDTA, 1% Nonidet P-40, 1 mM Na_3VO_4, 10 μg/ml aprotinin and leupeptin, 100 μg/ml soybean trypsin inhibitor, and 1 mM PMSF, pH 7.5, and clarified by centrifugation at 4000 × *g* for 20 min. The clarified lysates containing ~1 mg protein were preabsorbed on protein G-Sepharose and then incubated overnight with 10 μg anti-5-LO precipitating rabbit mAb or control IgG, followed by 2 h incubation with Protein A/G PLUS-Agarose beads. Immune complexes were extensively washed, suspended in Laemmli sample buffer and subjected to SDS/PAGE. Blots were stained to assess the protein present in the cell lysates used as starting material (input) and in the immunoprecipitates with anti-5-LO Ab (1:1000, v/v) and anti-P-Ser663-5-LO rabbit Ab (1:250, v/v) (Cell Signaling # 3749). For immunoblots directed to assay nuclear translocation of 5-LO, nuclear and cytoplasmic fractions were obtained by using a nuclear extract kit (Active Motif, Carlsbad, CA).

2.8. Assay of acetyl-CoA

This was addressed by an enzymatic end-point assay [19]. 15×10^6 DC were pelleted at 450 × *g* for 5 min, washed in 1 ml of cold PBS and lysed in 400 μl of hypotonic medium (5 mM Hepes, 1.5 mM $MgCl_2$, 10 mM KCl, 0.5% NP40, 50 mM NaF, 5 μg/ml leupeptin and 0.1 mM PMSF, pH 7.9) for 10 min on ice. Protein levels were determined spectrofotometrically and samples of 20 μl were mixed with 170 μl reaction buffer containing 100 mM Tris–HCl, 100 μM DTNB, (dithionitrobenzoic acid or Ellman's reagent), 1 mg/ml BSA, and 5 U of recombinant citrate synthase, pH 8.1. Optical density at 412 nm was measured as blank and then the reaction was initiated by adding 10 μl of oxalacetic acid 10 mM. The samples were incubated at 37 °C and the optical density was measured at 412 nm after 5 min using an ELISA plate reader.

2.9. Assays in the cell-free system

DC were incubated for 15 min at 37 °C at a density of 5×10^6 cells/ml and then stimulated with zymosan for 15 min. At the end of this period, DC were centrifuged for 5 min at 4 °C in precooled tubes containing in 0.1 M Tris–HC1, pH 7.4, and resuspended in the same medium. After two sets of 30s for cell disruption in a probe sonicator, the homogenate was used for the assay of LPCAT activity in the Tris–HCl medium supplemented with 0.2 μM $CaCl_2$ and 20 μM 1-hexadecyl-2-lyso-glycero-3-phosphocholine, in the presence and absence of 100 μM acetyl-CoA and 100 μM AA-CoA. The reaction was maintained at 37 °C for 30 min and stopped by adding 3.7 ml of chloroform/methanol (1:2) and Bligh and Dyer extraction. The organic phase was then removed, dried under N_2 stream, and lipids assayed by UPLC/MS.

2.10. Statistical analysis

Data are represented as the mean ± S.E.M. and were analyzed with the Prism 4.0 statistical program (GraphPad Software). Comparison between two experimental groups was carried out using the two-tailed Student's *t* test. Two-way ANOVA was used for comparison of two nominal variables, for instance, treatments at different times. Differences were considered significant for $p < 0.05$.

3. Results

3.1. Dectin-1, dectin-2, and lipid mediator receptors are involved in IL23A induction

Given that both the α-mannan and the β-glucan components of fungal cell wall cooperate to induce the host responses, we addressed whether the C-type lectin receptors dectin-1 and dectin-2 were involved in the induction of *IL23A* expression by using blocking antibodies. Both anti-dectin-1 and anti-dectin-2 Ab blunted the expression of *IL23A* mRNA significantly, whereas no inhibition was observed with an anti-CD11b Ab (Fig. 1A). When both anti-dectin-1 and anti-dectin-2 Ab were used in combination, the inhibition increased, although this only reached significance versus the inhibition induced by anti-dectin-1 Ab alone. This suggests that costimulation of β-glucan- and α-mannan-engaging receptors is required for a productive response [13,18,20]. Consistent with the signaling route of dectin-1 and dectin-2 via the tyrosine kinase SYK, the SYK inhibitor piceatannol induced an almost complete inhibition of *IL23A* mRNA expression. The $cPLA_2$ inhibitor pyrrolidine-1 and the 5-LO inhibitor zileuton also blunted the response, although their effects were less robust than the effect of piceatannol. In contrast, the 12/15-LO inhibitor EDC did not show any significant effect (Fig. 1B). Given that these results were consistent with the involvement of a signaling route downstream the tyrosine kinase SYK and the $cPLA_2$/5-LO routes, the role of LT was addressed. Neither montelukast nor U75302 inhibited *IL23A* mRNA expression significantly (Fig. 1C); however, this was observed using combination thereof. Since the release of AA by $cPLA_2$ may be coupled to PAF formation from the 1-alkyl-2-lyso-glycero-3-phosphocholine (lyso-PAF) resulting from the hydrolysis of 1-alkyl-2-arachidonoyl-*sn*-glycero-3-phosphocholine substrate and the incorporation of acetate into the *sn*-2 position of the

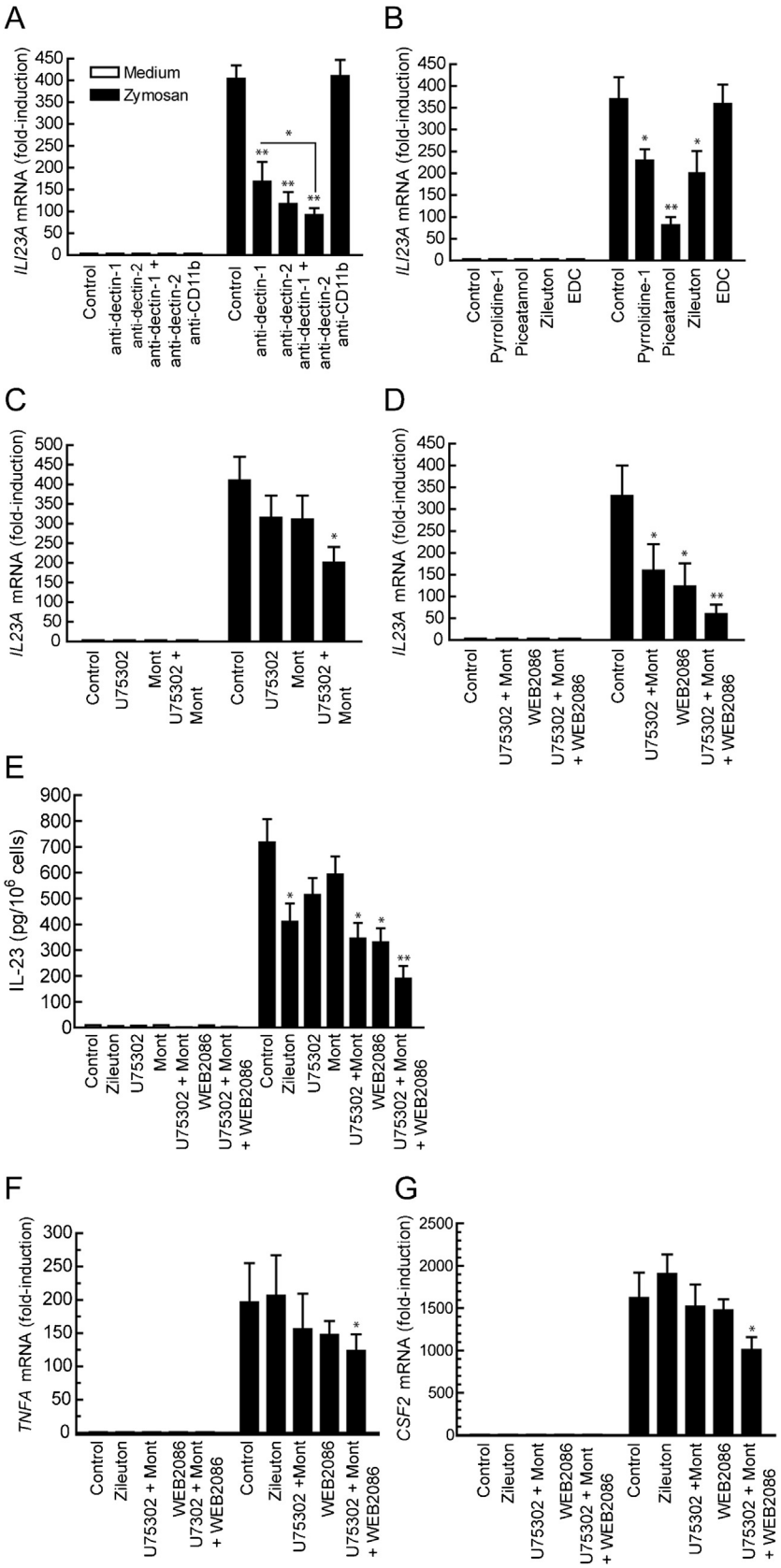

Fig. 1. Effect of different treatments on the induction of *IL23A*,*TNFA*, and *CSF2* mRNA. (A) DC were incubated for 30 min prior to the addition of 1 mg/ml zymosan with 10 μg/ml of either anti-dectin-1 or anti-dectin-2 Ab, and combination thereof. Anti-CD11b Ab was used as a control for specificity. Four hours after the addition of zymosan, the RNA was extracted and used for the assay of *IL23A* mRNA. (B–D) Similar experiments were carried out in the presence of the BLT1 antagonist U75302 1 μM, the CysLT1 antagonist montelukast 10 μM, the 5-LO inhibitor zileuton 10 μM, the 12/15-LO inhibitor EDC 3 μM, the phospholipase A_2 inhibitor pyrrolidine-1 2 μM, the SYK kinase inhibitor piceatannol 25 μM, and the PAF receptor antagonist WEB2086 30 μM. (E) Assay of IL-23 protein in supernatants of DC obtained after preincubation with different drugs and overnight stimulation with zymosan. (F and G) Effect of different treatments on the expression of *TNFA* and *CSF2*. Results show mean ± S.E.M. of three to six experiments. Mont indicates montelukast. $^{*}p < 0.05$, $^{**}p < 0.01$ as compared to control or anti-dectin-1 Ab versus combination of Ab.

glycerol backbone by LPCAT enzymes [21,22], the effect of the combined blockade of CysLT1, BLT1, and PAF receptor (PAFR) was assessed. *IL23A* mRNA expression was inhibited by 86% under these conditions (Fig. 1D), thus suggesting a cooperative effect of these receptors in the signalling route involved in *IL23A trans*-activation. Notably, the results on *IL23A* mRNA expression were also observed in ELISA assays of IL-23 protein, which showed a similar pattern of inhibition by compounds acting on the 5-LO and PAFR routes (Fig. 1E). Given that 5-LO function has been related to the dectin-1-dependent production of TNFα and GM-CSF [23], the expression of the mRNA encoding these cytokines was also assayed. In contrast to *IL23A* mRNA expression, the expression of *TNFA* and *CSF2* mRNA did not show significant changes in the sole presence of LT receptor antagonists, being a ~38% inhibition observed in both cases when the PAF receptor antagonist was included as well (Fig. 1F and G). These findings suggest a more prominent effect of the 5-LO route on the regulation of the p19 chain of IL-23 than on other cytokines robustly induced by zymosan.

IL23A expression induced by zymosan depends on at least the transcription factors NF-κB and ATF2, and SYK-dependent signals might play a role in the route that leads to the complementary phosphorylations of ATF2 and the binding to the *IL23A* promoter. On this basis, ChIP experiments were carried out using anti-P-71Thr-ATF2 Ab. Piceatannol, pyrrolidine-1, and zileuton induced a robust inhibition of P-71Thr-ATF2 binding to the *IL23A* promoter, whereas EDC did not show any significant effect (Fig. 2A). Attempts to address the role of mediators formed downstream the $cPLA_2$ showed a significant inhibition when BLT1 and CysLT1 were targeted, as well as a similar inhibition by the PAFR antagonist WEB2086 (Fig. 2B). When PAF and combination of LT were used, the binding of P-71Thr-ATF2 was increased, but it did not reach the levels observed in response to zymosan (Fig. 2C). Altogether, these data suggest the involvement of a signaling route involving C-type lectin receptors, SYK, $cPLA_2$, LT, and PAF in the induction of *IL23A* expression elicited by zymosan through a mechanism associated with ATF2 activation.

3.2. Assay of the eicosanoids generated in response to zymosan

Given that the pharmacological studies suggested the involvement of autocrine lipid mediators, the presence of eicosanoids was assayed by UPLC/MS. Zymosan induced a robust release of AA that reached levels above 1 μg/10^6 DC at one hour (Fig. 3A). Assay of the different eicosanoids showed a definite production of LTB_4, PGE_2, PGD_2, and 12-HETE, which was somewhat delayed as compared to the release of AA (Fig. 3B–E). These concentrations decreased to prestimulation levels at 24 h, with the exception of PGE_2 and PGD_2, which reached higher values at that time. In contrast, the levels of palmitic and stearic acids did not show any change in response to zymosan (peaks marked C16:0 and C18:0 in Fig. 4A), whereas the areas corresponding to oleic and docosahexaenoic acids showed small increases (peaks marked C18:1 and C22:6 in Fig. 4A, middle and lower panels). As expected, stimulation with zymosan in the presence of zileuton did not influence the release of AA significantly (Fig. 4A, middle panel). In contrast to the characterization of LTB_4, 12-HETE, and PGE_2, which could be identified by combination of mass spectra (Fig. 4B), the use of deuterated standards, and ion fragmentation patterns (Fig. 4C), the peak showing a *m/z* value of 438.2305 consistent with the $[M-H]^-$ ion of LTE_4 could not be quantified directly because it was not well separated from other compounds. Comparison of the different extraction procedures showed good recovery in most cases, except for LTB_4, which was best detected in samples containing BSA instead of FBS. Given that these experiments disclosed the presence of LTB_4 and LTE_4, which is the cysteinyl-LT resulting from dipeptidase action upon LTD_4, and this enzyme seems to be a

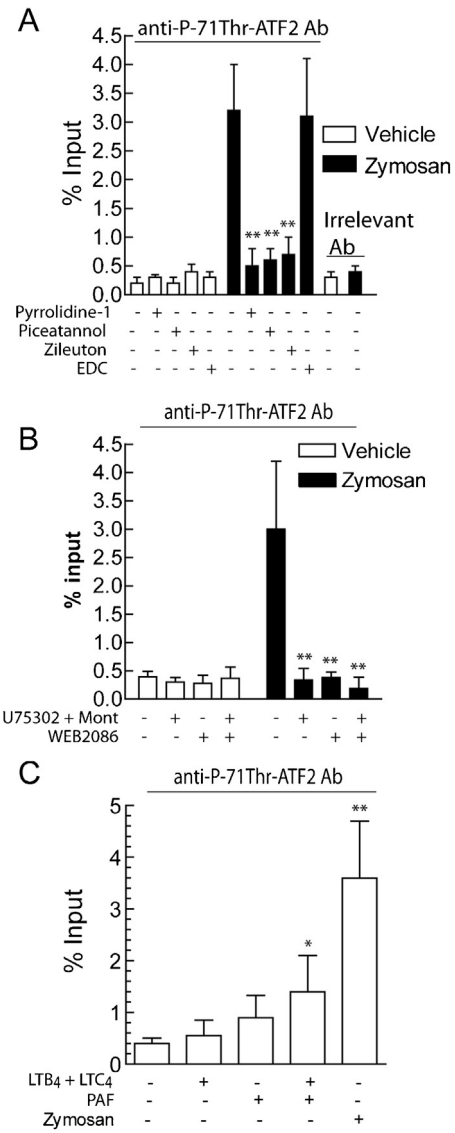

Fig. 2. Effect of compounds acting on the AA cascade on P-Thr71-ATF2 binding to the ATF2 site of the *IL23A* promoter. (A) DC were incubated with the indicated additions at the concentrations showed in the legend to Fig. 1 for 30 min, stimulated with 1 mg/ml zymosan for 1 h, and then collected for ChIP assays. Anti-P-71Thr-ATF2 and irrelevant control Ab were used at a concentration of 10 μg/ml. (B) Effect of 1 μM U75302 and 10 μM montelukast, 30 μM WEB2086, and combination thereof. (C) Effect of 0.1 μM LTB_4 and 0.5 μM LTC_4, 1 μM PAF, and combination thereof. Results show mean ± S.E.M. of three experiments. Mont indicates montelukast. $^*p < 0.05$. $^{**}p < 0.01$.

likely component of FBS, further assays were carried out using specific ELISA assays for LTE_4 and LTB_4. LTE_4 was detected at a concentration of ~7 ng/10^6 cells, which agrees with the concentration at which its immediate precursor LTD_4 is most active on the CysLT1 receptor [24]. A significant production was also observed in response to heat-inactivated *Candida* (Fig. 5A). The assay of LTB_4 showed lower concentrations, ~2 ng/10^6 cells, but this concentration fits well with that inducing responses in granulocytes. Whereas the different components of fungal patterns induced LTE_4 production, LTB_4 was only detected in response to zymosan and *Candida* (Fig. 5B). Unlike EDC, piceatannol and zileuton blunted the production of LTE_4 and LTB_4 (Fig. 5C and D). The involvement of dectin-1 and dectin-2 was confirmed with blocking Ab. Combined Ab showed an additive effect in the case of LTE_4, whereas the release of LTB_4 was almost completely inhibited by the

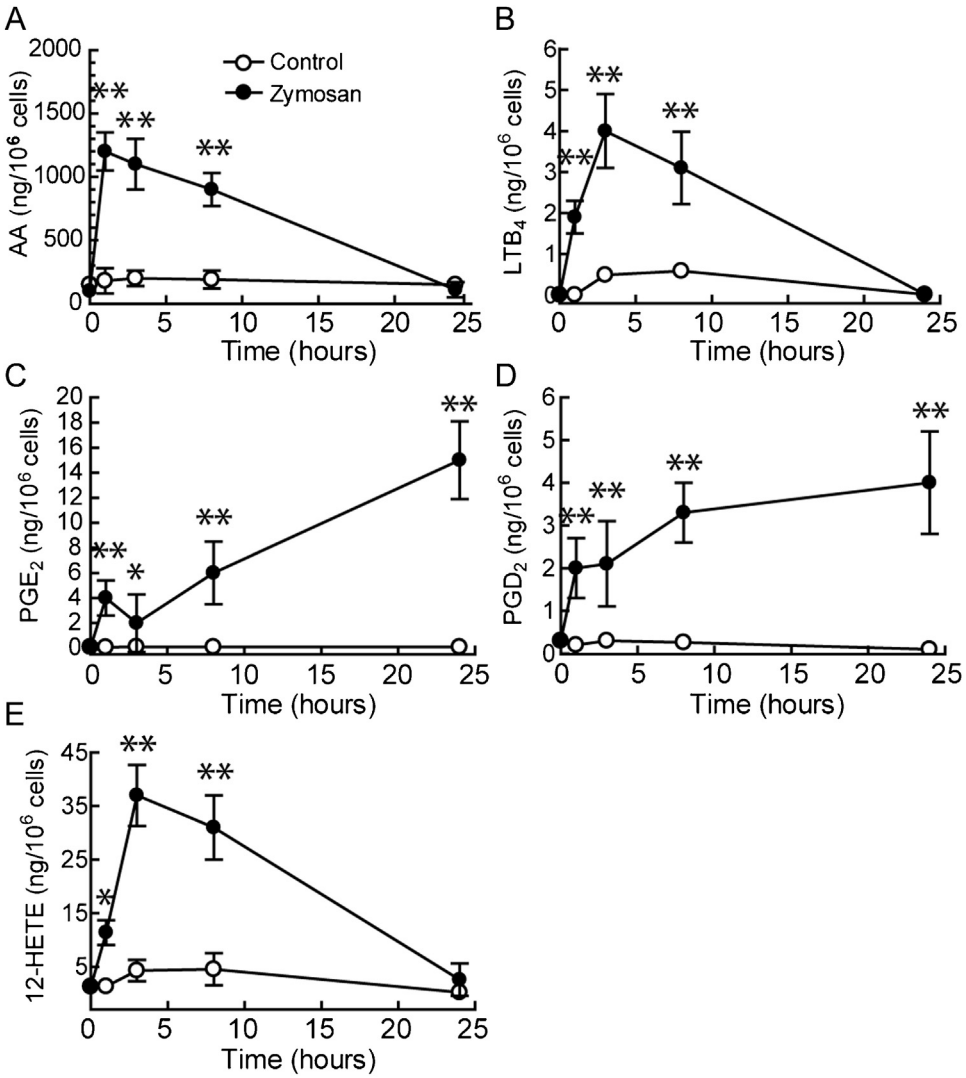

Fig. 3. Production of eicosanoids in response to zymosan. (A–E) DC were incubated for the times indicated in the presence and absence of 1 mg/ml zymosan, and the supernatants collected at the end of these periods for lipid extraction in C-18 reversed-phase cartridges and assay of eicosanoid production by UPLC/MS assay. Results show mean ± S.E.M. of 4 independent experiments. $^{*}p < 0.05$. $^{**}p < 0.01$.

anti-dectin-1 Ab (Fig. 5E and F). Consistent with the production of LT, DC showed a robust expression of 5-LO in immunofluorescence confocal microscopy (Fig. 5G) and DC lysates (Fig. 5H), as well as some evidence of its activating phosphorylation on Ser663 (Fig. 5H) and possible nuclear translocation (Fig. 5I), although its detection may be hampered by the changes of the cytoskeletal structure induced by the phagocytic challenge (Fig. 5G). These results point at the involvement of LT in the transcriptional regulation of *IL23A* and agree with the well-known effect of their cognate receptors on the activation of protein phosphorylation cascades.

3.3. Role of 5-LO and PAF in the trans-activation of IL23A

Taking into account the result of the pharmacological experiments with receptor antagonists and the production of LT by DC, the effect of exogenous LT and PAF on *IL23A* mRNA expression was assessed. The usage of 0.1 μM LTB_4 and 0.5 μM LTC_4 did not enhance the induction of *IL23A* mRNA expression produced by zymosan (not shown), which most likely indicates that these mediators were produced at concentrations high enough to elicit their effects. To further address this mechanism, exogenous eicosanoids and the lipid extract of zymosan-stimulated DC were used in combination with LPS, a stimulus that does not induce robust activation of the $cPLA_2$ route [25], only drives changes of the eicosanome with a delayed onset [17], and is a less potent stimulus than zymosan to *trans*-activate the *IL23A* promoter [7]. The lipid extract from the conditioned medium of DC stimulated for one hour with zymosan increased the induction of the mRNA of both *IL23A* and *IL10* elicited by LPS (Fig. 6A and B), thus suggesting the presence of lipid mediators. In contrast, the lipid extract from DC stimulated for 24 h did not show any effect. In the case of *IL23A*, this increase showed a similar trend to that observed in DC stimulated with LPS in the presence of a combination of 1 μM PAF, 0.1 μM LTB_4, and 0.5 μM LTC_4 (Fig. 6C), whereas the only addition of PAF mimicked the effect observed on *IL10* mRNA induction expression (Fig. 6D), thus agreeing with the notion that the effect of PAF may involve the secondary formation of other mediators [26]. Taken together, these results suggest that unlike LPS, zymosan elicits the generation of lipid mediators to an extent as high as to allow an optimal *trans*-activation of *IL23A* and disclose an autocrine effect of PAF and LT on the transcriptional up-regulation of *IL23A*, which can be explained by an array of signals from at least three different types of G protein-coupled receptors.

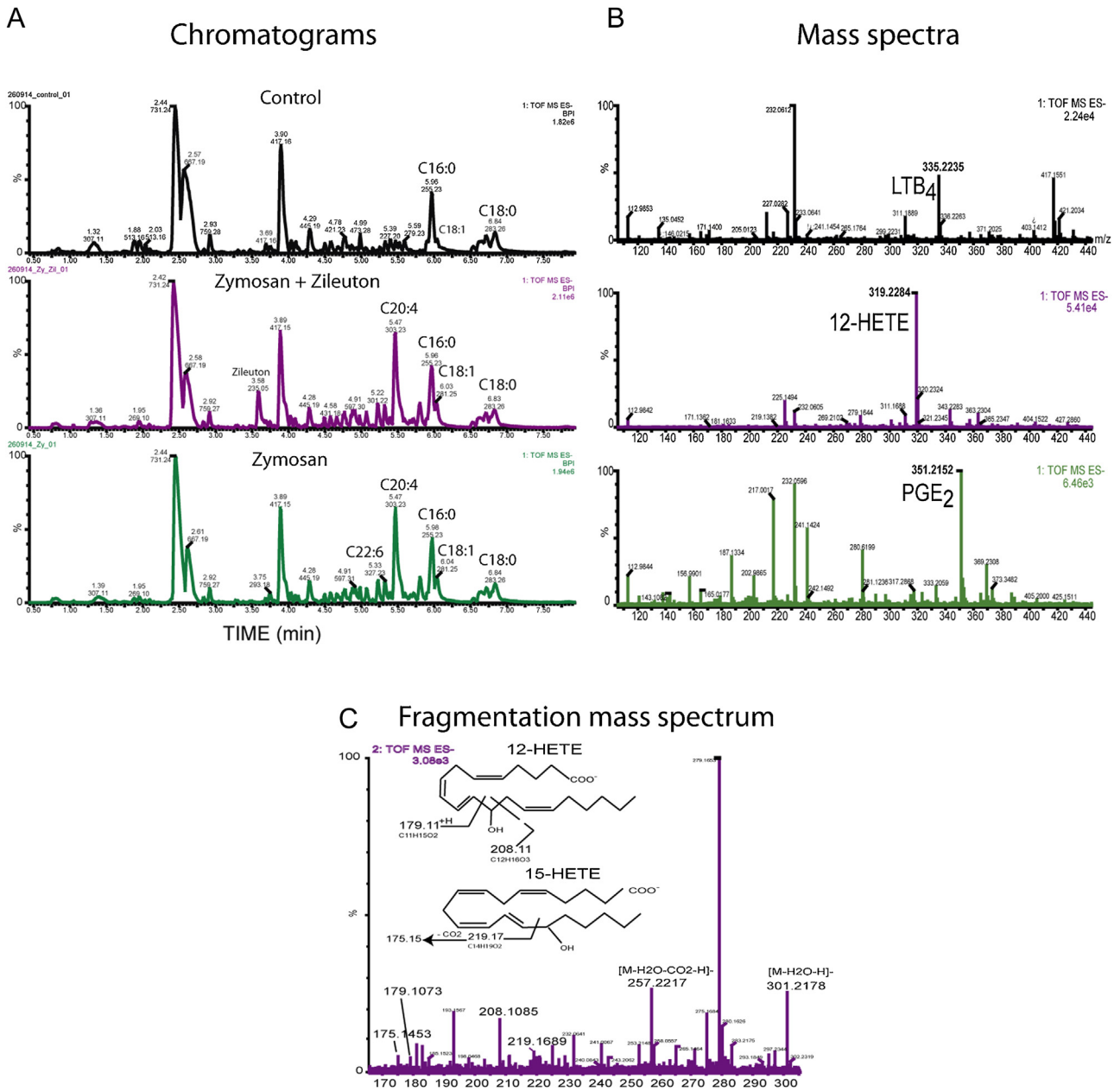

Fig. 4. Lipid extract analysis of DC conditioned media and MS characterization of the eicosanoids released by DC. (A) The culture medium of resting DC and DC stimulated for one hour with zymosan in the absence and presence of zileuton was extracted in C-18 reversed-phase cartridges and used for UPLC/MS assays. C16:0, C18:0, C20:4, C18:1, and C22:6 refer to palmitic acid, stearic acid, arachidonic acid, oleic acid, and docosahexaenoic acid, respectively. Chromatograms are representatives of 4 experiments for control and zymosan and 2 experiments in the case of zymosan + zileuton. (B) Mass spectra of the eicosanoids released by DC. (C) High energy (fragmentation) mass spectrum used to characterize 12-HETE, showing the typical product ions of *m*/*z* 179 and 208. The product ions of *m*/*z* 175 and 219 correspond to a small amount of 15-HETE.

3.4. *Effect of* PGE_2 *on* IL23A *regulation*

Recent reports have disclosed a synergistic effect of exogenous PGE_2 on the transcription of *IL23A* elicited by LPS and TNFα through a route involving EP/cAMP/PKA and the cooperation of CREB and C/EBPβ with NF-κB proteins [9]. Since both ATF2 and CREB are transcription factors sensitive to the intracellular levels of cAMP and PKA activity, some experiments were conducted to address the mechanism whereby PGE_2 might exert its effect on *IL23A* and *IL10* expression. The rationale behind these experiments was that IL-10 is an outstanding component of the set of cytokines induced by zymosan, the regulation of which is fine-tuned by the EP/cAMP/PKA/CREB cascade [18,27,28]. On this basis, the parallel assay of both cytokines helps disclose differences in their transcriptional regulation. Incubation of DC with both the cell permeable cAMP analogue 8-Br-cAMP and PGE_2 did not induce *IL23A* and *IL10* mRNA, but enhanced the response elicited by either LPS or zymosan (Fig. 7A and B). This effect being more prominent on the induction of *IL23* mRNA induced by zymosan. Conversely, PGE_2 inhibited the expression of *IL12B* to a larger extent in LPS-treated DC, i.e., 95%, versus a 33% inhibition in the case of zymosan (Fig. 7C), thus agreeing with both a stimulus-specific effect of PGE_2 and the notion that the effect of PGE_2 can not be only assigned to the PKA route [29]. COX-1 and COX-2 inhibitors did not affect the expression of *IL23A* mRNA in response to both LPS and zymosan, provided the concentrations of these inhibitors were maintained at levels consistent with the preservation of their selectivity (Fig. 7D). In contrast, *IL10* mRNA expression was reduced in response to both

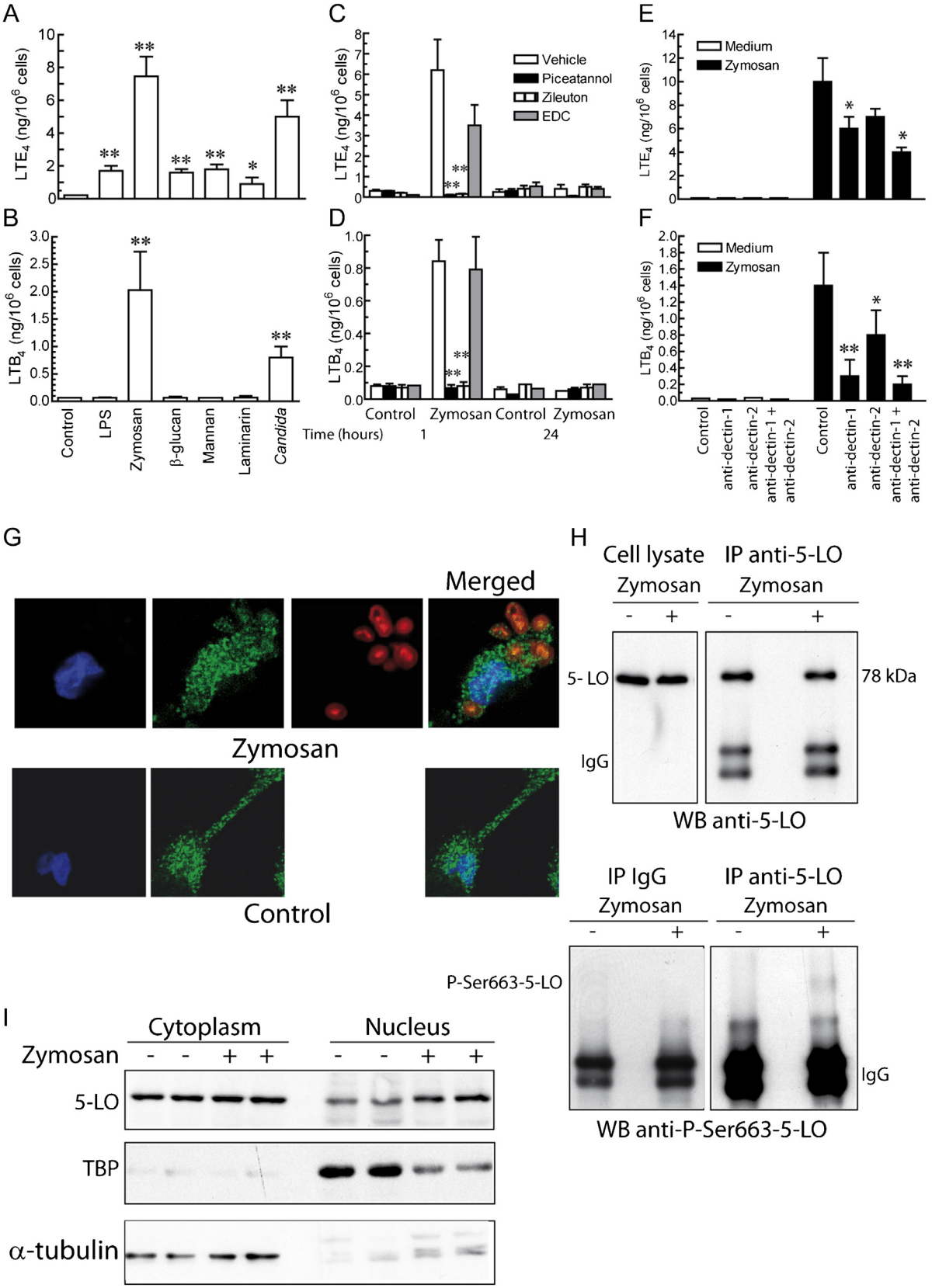

Fig. 5. Production of LTB_4 and LTE_4 by DC and effect of pharmacological treatments. (A–F) DC were incubated with 10 μg/ml LPS, 1 mg/ml of the different zymosan components, and with *Candida* at a ratio of 50 conidia per DC. The supernatants were collected at the times indicated for the ELISA assay of LT. The effect of compounds acting on SYK, 5-LO and 12/15-LO, and blocking Ab acting on dectin-1 and dectin-2 was assessed by incubating the DC in the presence of the indicated additions for 30 min prior to zymosan addition. Concentrations were as described in the legend to Fig. 1. (G) Immunofluorescence confocal microscopy of 5-LO (green staining) in control DC and in DC incubated for 30 min with zymosan particles (red staining). DAPI was used to stain the nuclei (blue staining). (H) Expression of 5-LO in cell lysates and its phosphorylation in Ser663 in an immunoprecipitation assay in DC stimulated for 15 min with zymosan. (I) Location of 5-LO in the cytoplasm and nucleus of DC stimulated for 1 h with zymosan.

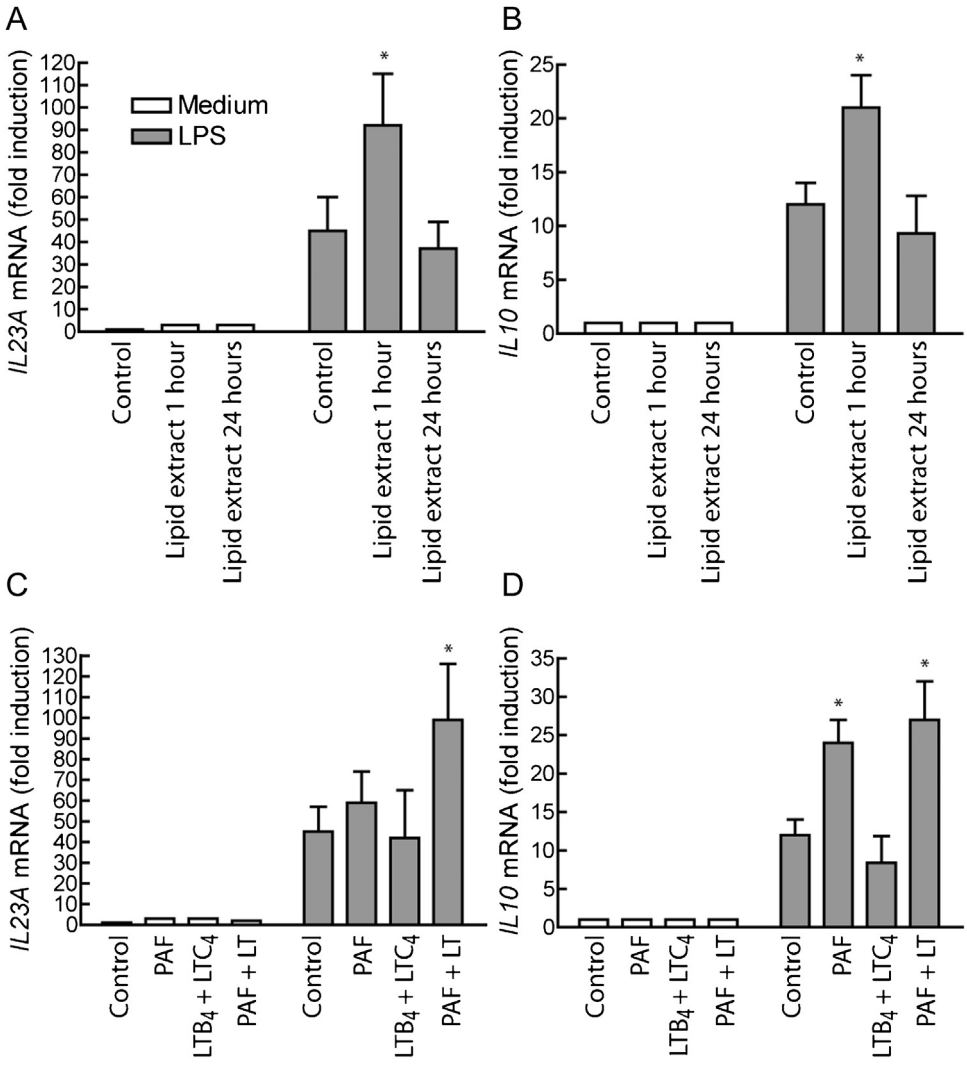

Fig. 6. Effect of the lipid extract from conditioned medium and exogenous lipid mediators on the mRNA expression of *IL23A* and *IL10* in response to LPS. (A and B) DC were stimulated in the presence of 1 mg/ml zymosan for 1 or 24 h. At the end of these times, the supernatants were collected and their lipid fractions extracted in C-18 reversed-phase cartridges. The lipid extract was evaporated to dryness, resuspended in culture medium (lipid extract 1 h and lipid extract 24 h in the legend) and used to address its effect on the response elicited by LPS. After 4 h of incubation in the presence of 10 μg/ml LPS, the RNA was extracted and used for the assay of the mRNA of the cytokines. (C and D) The effect of the addition of exogenous lipid mediators on the expression of *IL23A* and *IL10* mRNA was assayed in DC stimulated for 4 h in the presence of LPS. The concentrations of the lipid mediators are 0.1 μM LTB_4, 0.5 μM LTC_4, and 1 μM PAF. Results show mean ± S.E.M. of 4 independent experiments. $^{*}p < 0.05$.

stimuli, although the effect observed following stimulation with zymosan was more robust (Fig. 7E). Unlike COX-1 inhibition, the COX-2 inhibitor sc-236 strongly inhibited *IL12B* mRNA induction in response to both LPS and zymosan (Fig. 7F), thus suggesting that the delayed production of prostaglandins via COX-2 might play an autocrine role in *IL12B* expression. In order to associate the effect of PGE_2 on *IL23A* expression with the activation of transcription factors, binding of P-71Thr-ATF2 and P-133Ser-CREB to their regulatory sites in the *IL23A* promoter was addressed. PGE_2 increased the binding of P-71Thr-ATF2 to the ATF2 site in response to both zymosan and LPS (Fig. 7G), thus suggesting that a portion of PGE_2 effect might be exerted via ATF2. PGE_2 also enhanced the binding of P-Ser133-CREB to the CRE site elicited by zymosan. Taken together, these results suggest that paracrine PGE_2 synergizes with zymosan to induce *IL23A* and *IL10* mRNA, and that autocrine PGE_2 plays a significant role in *IL10* induction in response to both LPS and zymosan, and in the *IL23A* response elicited by LPS. The effect of paracrine PGE_2 on *IL23A* expression can be explained through the activity of two cAMP-regulated transcription factors, ATF2 and CREB.

3.5. PAF production by DC

PAF is produced in parallel to eicosanoids by acetylation of lyso-PAF by LPCAT2, a Ca^{2+}-dependent enzyme that is activated by the PKCα isoform [30] and the p38 MAPK/MAPK-activated protein kinase 2 (MK2)-dependent pathway [31]. Although PAF formation was a likely event in our system, the presence of FBS in the medium made it difficult its detection because PAF-acetylhydrolases are present in cells and serum [32]. Given that LPCAT enzymes are a family of proteins involved in phospholipid remodeling, triglyceride secretion, and PAF biosynthesis that show a tissue-specific

TBP indicates TATA box-binding protein. Comparison were made in control versus stimulus-treated samples in (A) and (B), in vehicle versus treatment in zymosan-stimulated samples in (C) and (D), and in control versus samples treated with 10 μg of anti-dectin-1 and anti-dectin-2 Ab in (E) and (F). IP indicates immunoprecipitation. WB indicates Western blot. Results show mean ± S.E.M. of 3 independent experiments. $^{*}p < 0.05$. $^{**}p < 0.01$.

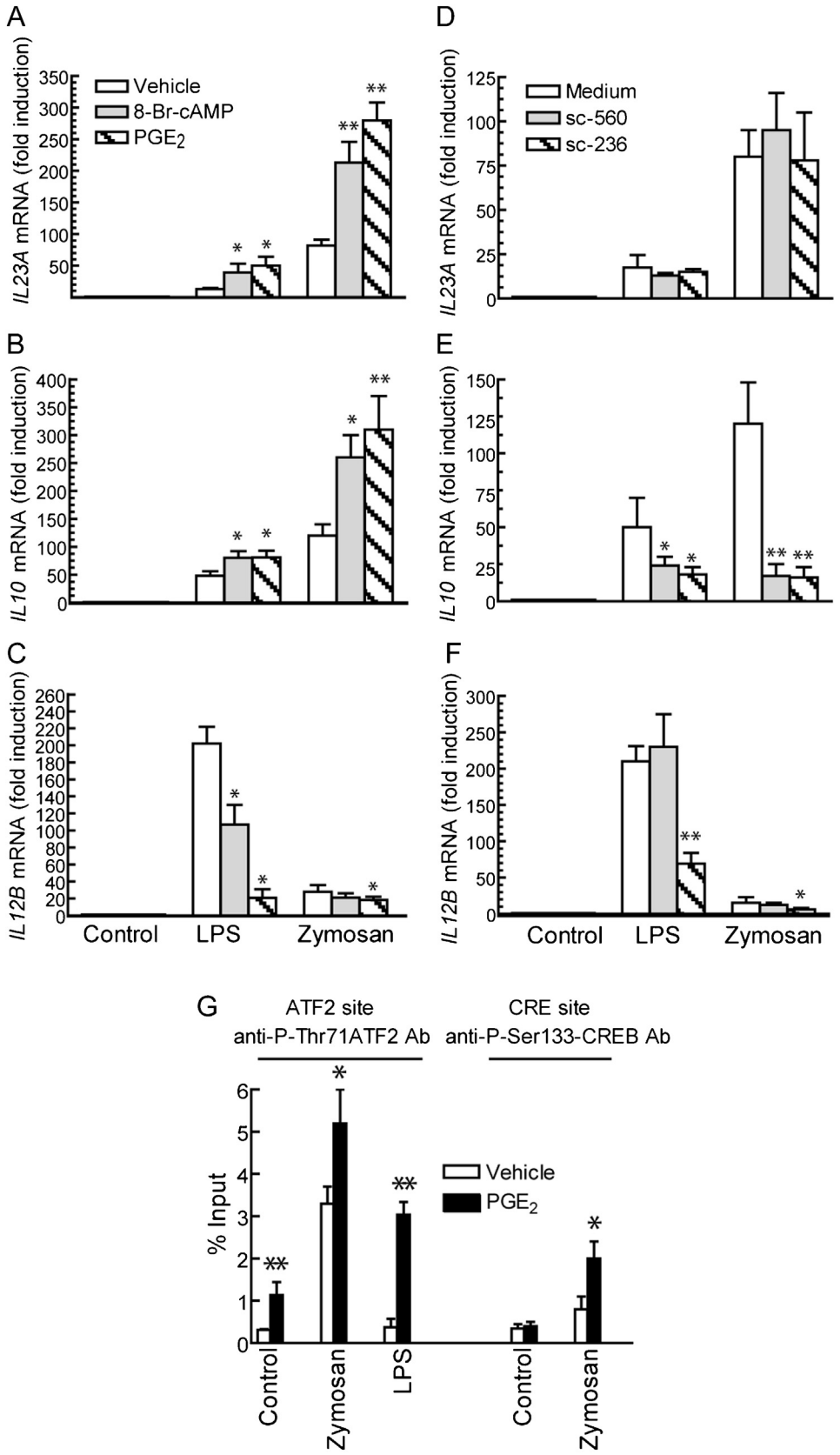

Fig. 7. Effect of 8-Br-cAMP, PGE_2, and COX inhibitors on cytokine expression. (A–C) DC were incubated with 8-Br-cAMP and PGE_2 for 30 min prior to the addition of the stimuli and after 4 h, cells were collected for the assay of the mRNA encoding the different cytokines. (D–F) Effect of the selective inhibitors of COX-1 (50 nM sc-560) and COX-2 (50 nM sc-236) activities. (G) Effect of the preincubation with 1 μM PGE_2 prior to the stimulation with zymosan and LPS on the binding of P-Thr71-ATF2 and P-Ser133-CREB to their cognate sites in the *IL23A* promoter. The results represent mean ± S.E.M. of 3–5 experiments. $^{*}p < 0.05$. $^{**}p < 0.01$.

pattern of expression [33], their mRNA levels were assayed. Transcripts encoding *LPCAT1*, *LPCAT2*, and *LPCAT3* were detected over the process of differentiation of DC. *LPCAT2* and *LPCAT3* mRNA were expressed in the same range, whereas the expression of *LPCAT1* was lower (Fig. 8A). Both *LPCAT2* and *LPCAT3* enzymes showed a trend to decrease at 8–16 h after zymosan challenge (Fig. 8B). The production of PAF by LPCAT activity was confirmed in the cell-free medium in the presence of both lyso-PAF and acetyl-CoA. When AA-CoA was used as a co-substrate, a partial inhibition of PAF formation was observed (Fig. 8C). The assay of acetyl-CoA levels in the lysates of DC stimulated with zymosan showed a decrease at one hour, an increase at 3 h, and a new reduction at 6 h (Fig. 8D), thus suggesting the occurrence of an early consumption of acetyl-CoA, followed by an increased generation most likely related to increased aerobic glycolysis [34]. The involvement of PAF in DC responses was also supported by the expression of the mRNA encoding the PAFR (*PTAFR* gene, transcript variants 1 and 3, Fig. 8E), which agrees with earlier reports showing functional PAFR in DC [35]. Initial MS assays showed PAF C18:0 at low concentrations and a robust production of lysophosphatidylcholines (LPC) in the cell supernatants (Table 2). Taking into account that the presence of PAF-acetylhydrolase could be a drawback for the assays, experiments were conducted in the presence of the PAF-acetylhydrolase inhibitor darapladib 0.1 μM. Under these conditions, PAF C16:0 was detected in resting cells and at significantly higher levels after zymosan stimulation (Table 2 and Fig. 8F and G). Given that PAF C18:0 was not detected consistently, several hypotheses were put forward: (i) preferential production of the C16:0 species, (ii) retention on the cell membranes, and (iii) inefficient extraction. Experiments showed that PAF C18:0 was not detected in the cell pellets nor in supernatants subjected to Bligh and Dyer extraction. In contrast, an efficient recovery of PAF C18:0-d4 was obtained from cell supernatants after addition of the standard, thus suggesting that cell retention of PAF C18:0 does not occur under the conditions of the assay and that DC mainly produce PAF C16:0.

3.6. ALOX12 *and* ALOX15 *expression and metabolism of AA-CoA in the cell-free system*

In keeping with previous reports [36,37], the expression of *ALOX15* (12/15-LO gene) mRNA was very high over the differentiation process, whereas that of *ALOX12* was extremely low (Fig. 9A). Given the robust expression of the mRNA encoding *LPCAT* and *ALOX* enzymes, functional assays were carried out in the cell-free system using the exogenous substrates used for LPCAT activity assays. The analysis of products derived from AA-CoA showed a robust formation of unesterified AA, 12-HETE and 15-HETE (Figs. 9 B and C and 10 A–C). Notably, 15-HETE, which was hardly detectable in the DC supernatants, was found along with 12-HETE in the cell-free system, whereas PGE_2 and LTB_4 were detected at lower concentrations (Fig. 9C). These results agree with the high expression of *ALOX15* mRNA and suggest the presence of robust acyl-CoA thioesterase activity as well.

Table 2
Production of PAF and LPC.

	Control	Zymosan
PAF C16:0 (ng/10^6 cells)	6 ± 3	89 ± 25
PAF C18:0 (ng/10^6 cells)	0.046	0.14
LPC C16:0 (ng/10^6 cells)	N.D.[a]	126 ± 36
LPC C18:1 (ng/10^6 cells)	N.D.	98 ± 28
LPC C20:4 (ng/10^6 cells)	N.D.	53 ± 16

DC were stimulated for 1 h with 1 mg/ml zymosan and the lipid extract was taken for the assay of PAF and LPC species. PAF C16:0 was detected in the presence of 0.1 μM darapladib as shown in a typical experiment in Fig. 8F. These are results from 3 independent experiments where PAF C16:0 was detected and from a typical experiment where PAF C18:0 was detected.

[a] N.D.: not detected.

4. Discussion

The present data underscore the role of lipid mediators in the regulation of the expression of cytokines induced by fungal patterns. Previous studies showed the dependence of *IL10* expression on autocrine PGE_2 and another report disclosed a role of LTB_4 as an autocrine self-amplifying loop necessary for the production of IL-12 p40, TNFα, and GM-CSF in peritoneal macrophages stimulated with curdlan, a hardly soluble pure β-glucan stimulus that lacks the structure of the fungal cell wall [23]. Our data unveil new mechanistic details on transcriptional regulation because *TNFA* and *CSF2* expression mainly depends on NF-κB [38], whereas *IL23A* expression requires at least ATF2 and NF-κB proteins. In addition to the distinct regulation of *IL23A* expression by latent transcription factors, our focus on IL-23 is explained by its central role in the maintenance of the Th17 response, the defense against fungal invasion, and the development of autoimmunity.

The results show a cooperative model where the generation of LT and PAF teams up to promote the phosphorylation-dependent activation of ATF2 and its ensuing cooperation with NF-κB proteins to *trans*-activate *IL23A*. These findings disclose a paradigm where a set of autocrine mediators that activate G protein-coupled receptors and phospholipase Cβ [39] enhance the phosphorylation reactions and the mobilization of Ca^{2+} initiated by the receptors engaged by fungal patterns, which activate phospholipase Cγ (Fig. 11). Pharmacological treatments showed a different degree of efficacy depending on the position of their targets in the route. For instance, the SYK kinase inhibitor piceatannol was more effective to inhibit LT biosynthesis than AA release. A plausible explanation is that tyrosine phosphorylation reactions are necessary, not only to activate $cPLA_2$, but also to phosphorylate 5-LO [40] and the 5-LO activating protein FLAP [41]. The inhibition of *IL23A* mRNA expression induced by the receptor antagonists was somewhat lower than the effect on P-71Thr-ATF2 binding to the *IL23A* promoter, which may be due to the recruitment of another transcription factor, for instance CREB, or by a remaining P-69Thr-ATF2 phosphorylation.

Zymosan induced a massive release of AA that was only partially processed in the oxidative metabolism. This suggests unique properties of DC as compared to other cells [42,43]. The high turnover of AA may improve the endocytic function, since remodeling the membrane with polyunsaturated fatty acids reduces the energetic cost of phagocytosis [44]. Moreover, the differentiation induced by GM-CSF endows DC with a set of C-type lectin receptors to carry out non-opsonic phagocytosis and increases the expression of PPARγ, which is a key transcription factor for the control of lipid metabolism [45]. One explanation for the limited rate of AA oxidative metabolism can be that zymosan also controls 5-LO and LTC_4 synthase activities to keep LT in levels consistent with appropriate homeostasis. In fact, phosphorylation of 5-LO at Ser523 by PKA suppresses its catalytic activity [46] and prevents its nuclear localization [47]. Phosphorylation of Ser271, which is very prominent in *in vitro* assays [40], only seems functionally relevant under conditions that do not increase intracellular Ca^{2+} robustly [48]. Zymosan also suppresses LTC_4 synthase activity via kinases, for instance PKA [49]. Given that fungal patterns activate PGE_2 biosynthesis and PKA activity, the existence of some degree of blockade of the 5-LO route under these conditions seems plausible and agrees with the limited evidence of Ser663-5-LO phosphorylation and 5-LO nuclear translocation.

The robust detection of 12-HETE can be explained by the strong expression of *ALOX15*. The predominant formation of 12-HETE in the supernatants was unexpected, but was confirmed by the

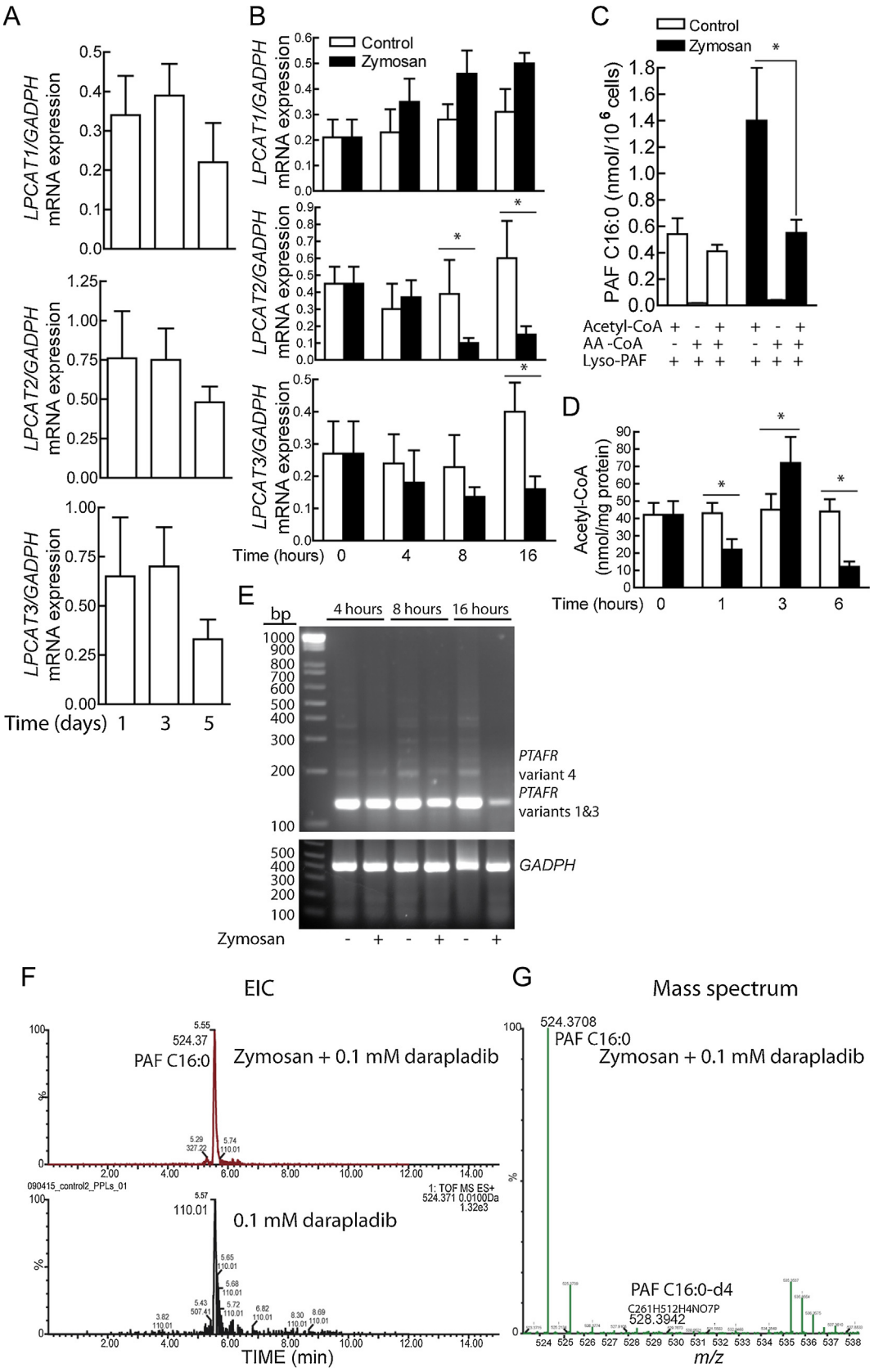

Fig. 8. Induction of the mRNA encoding *LPCAT1-3*, PAF production, and *PTAFR* expression. (A) Monocytes were cultured in the presence of GM-CSF and IL-4 for the days indicated and used for the assay of the mRNA encoding LPCAT enzymes. (B) DC we incubated in the presence and absence of zymosan for the times indicated and then used for the assay of mRNA encoding the different enzymes. (C) LPCAT activity was assayed in the cell-free system in homogenates of both resting and zymosan-treated DC using 20 μM 1-hexadecyl-2-lyso-glycero-3-phosphocholine and 100 μM acetyl-CoA or 100 μM AA-CoA or combination thereof as indicated. The lipid extract was used for the UPLC/MS assay. (D) Acetyl-CoA was assayed in DC lysates at different times after addition of zymosan. (E) The expression of the mRNA encoding the *PTAFR* was assayed by conventional RT-PCR with two forward primers and a reverse primer to address the expression of the different transcript variants at different times after zymosan challenge.

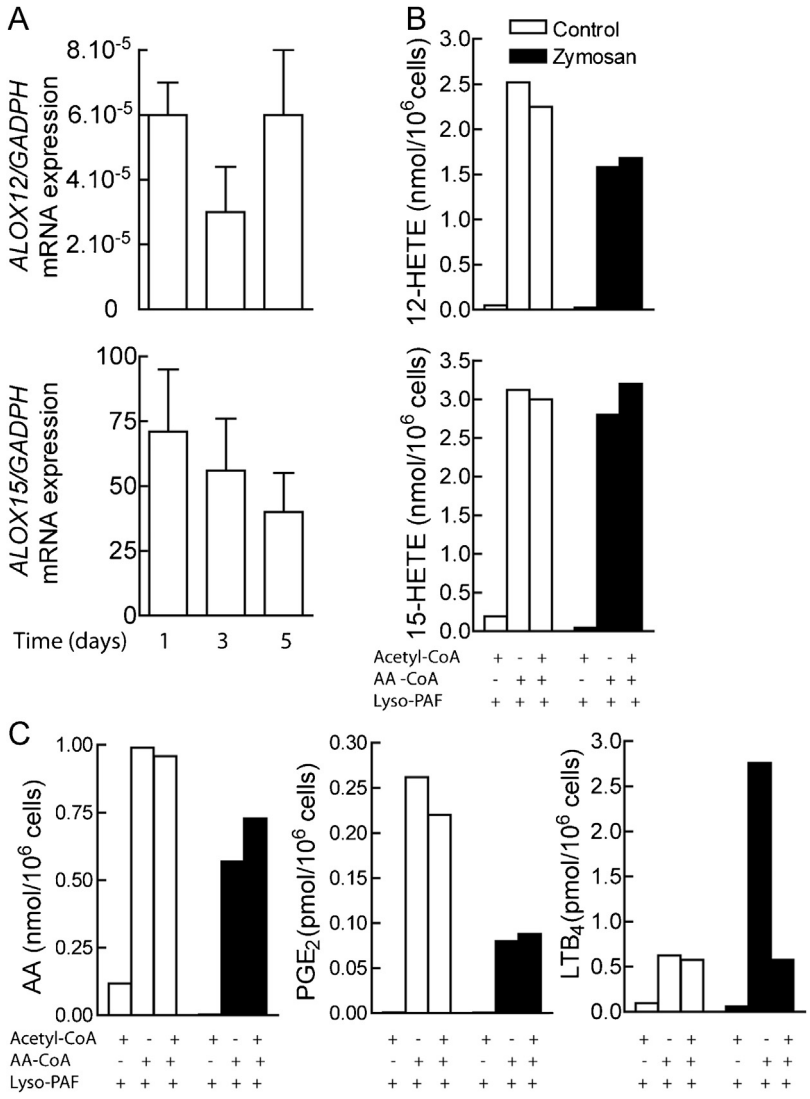

Fig. 9. Expression of the mRNA encoding *ALOX12* and *ALOX15* and assay of AA-CoA derived products in the cell-free system. (A) Monocytes were cultured in the presence of GM-CSF and IL-4 for the days indicates and used for the assay of the mRNA encoding *ALOX12* and *ALOX15*. Results represent mean ± S.E.M. of 3 experiments. (B and C) 12-HETE, 15-HETE, unesterified AA, PGE_2, and LTB_4 were assayed by UPLC/MS in homogenates from resting and zymosan-stimulated DC supplemented with lyso-PAF, acetyl-CoA, and AA-CoA at the concentrations indicated in the legend to Fig. 8C.

absence of significant amounts of 12,15-diHETE and the detection of the typical product ions of *m*/*z* 208 and 179 in the fragmentation mass spectrum (Fig. 4C). Given that assays in cell extracts showed the conversion of AA-CoA into both 12-HETE and 15-HETE, a different production of regioisomers from free and esterified AA substrates seems likely. 12/15-LO-oxygenated phospholipids have been found to reduce *IL23A* expression and control DC maturity in response to LPS [37], whereas under our experimental conditions inhibition of 12/15-LO did not show any significant effect on *IL23A* expression. This can be explained by mechanistic differences since the purported sequence of events in our model is $cPLA_2$/LO, whereas in the case of LPS, 12/15-LO oxygenated phospholipids are first produced and the generation of free eicosanoids requires another stimulus that mobilizes Ca^{2+}, activates $cPLA_2$, and releases both AA and 15-HETE [50].

The pharmacological effect of BLT1 and CysLT1 antagonists was enhanced in the presence of a PAFR antagonist. This is consistent with a mechanism whereby combined engagement of BLT1, CysLT1, and PAFR provides a set of signals dependent on distinct Gα protein subunits. BLT1 signaling is strongly dependent on a $G\alpha_{16}$ subunit [51], which activates Ras and the heterodimerization of cRaf and BRaf [52,53], as well as on $G\alpha_i$, which activates PLCβ and PKC. The PAF [54] and the CysLT1 receptors [55,56] signal via $G\alpha_q$ and $G\alpha_i$ to protein kinase C and this leads to Raf activation [57,58] (Fig. 11). Notably, it has been reported most recently the involvement of $G\alpha_i$ nucleotide exchange and Ca^{2+} transients in the uptake of zymosan

The expression of the mRNA encoding the enzymes is expressed as the ratio to *GADPH* to allow a comparison of their distinct expression levels in resting cells differentiated in the presence of GM-CSF and IL-4 for the indicated days or at different times after zymosan stimulation. (F) DC were incubated in the presence of 0.1 μM darapladib for 30 min and in the presence or absence of zymosan for one hour. At the end of this time, the deuterated standards were added to the supernatants. The extracted ion chromatogram (EIC) of PAF C16:0 is shown using different scales. In the absence of zymosan the EIC only clearly shows a 110.01 *m*/*z* compound. (G) Mass spectrum corresponding to zymosan-treated DC. The peaks of the *m*/*z* for deuterated and endogenous PAF C16:0 are indicated. Results represent mean ± S.E.M. of 3 experiments for the assay of the mRNA of the enzymes and PAF C16:0 (panels A–C), and 4 independent experiments for acetyl-CoA assay. $^*p < 0.05$. EIC are representative of 3 independent experiments.

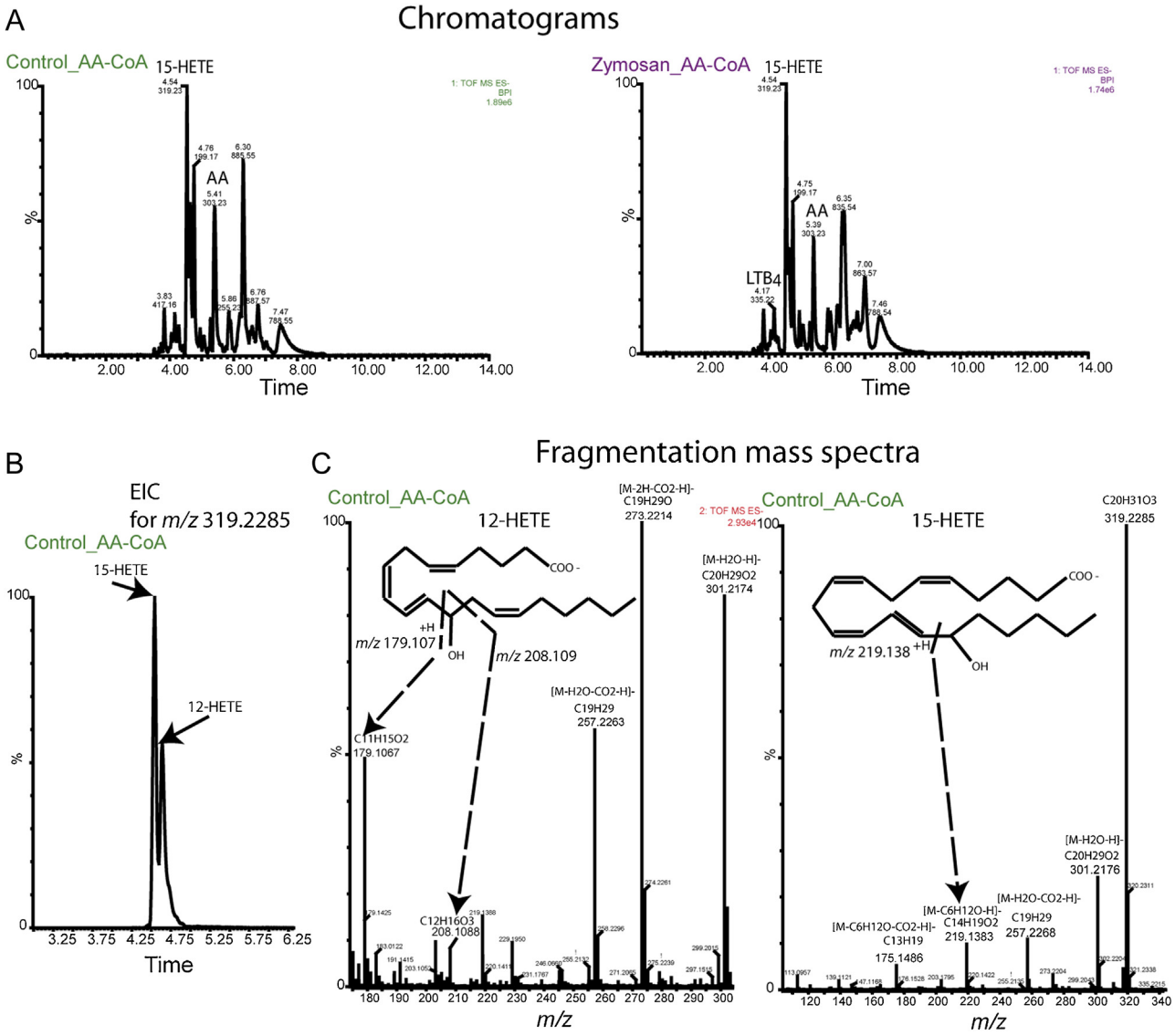

Fig. 10. Analysis of the lipid extract of cell-free media supplemented with AA-CoA. (A) DC at the concentration of 5×10^6/ml were incubated for 15 min at 37 °C in the presence or absence of zymosan. At the end of this period, DC were sonicated and the cell-free media were supplemented with 20 μM 1-hexadecyl-2-lyso-3-glycerophosphocholine and 100 μM AA-CoA. After 30 min, the reaction was stopped by Bligh and Dyer extraction and the lipid extract used for UPLC/MS analysis. Chromatograms showing the presence of unesterified AA, 12-HETE, 15-HETE, and LTB_4 in the zymosan treated sample are shown. (B) EIC showing the separation of 12-HETE and 15-HETE. (C) Fragmentation mass spectra showing the presence of both 12-HETE and 15-HETE.

particles [59]. Although the underlying mechanism was not disclosed, the rapid occurrence of Ca^{2+} transients and its inhibition by pertussis toxin is consistent with the involvement of BLT1, CysLT1, and PAFR.

The analysis of the COX/PGE_2/PKA route on *IL23A* regulation has been focussed on the results of pharmacological experiments. PKA activates CREB and this explains the synergistic effect of exogenous PGE_2 on the response to LPS [60] and TNFα [9]. However, the actual involvement of this route as an autocrine feed-forward loop has not been proved unambiguously for all of the stimuli. For instance, COX inhibition by indomethacin showed a weak inhibitory effect [9] and we failed to inhibit *IL23A* induction expression by both COX-1 and COX-2 inhibitors. This agrees with studies underscoring the cell type-dependent effect of PGE_2, which is explained by the distinct distribution and functional properties of the EP receptors. We further addressed this issue using EP selective agonists and antagonists, but unlike the results on *IL10* mRNA induction, we observed inconsistent results that could be explained taking into account that partial inhibition of COX activities and low concentrations of PGE_2 may channel the agonists into receptors with higher affinities, for instance EP3 and EP4, whereas a strong inhibition of COX activities blocks all the receptors. In keeping with this view, PGE_2 inhibited the production of both IL-12 p70 and IL-23 in human monocytes and slightly enhanced IL-23 production in DC [11]. A comprehensive study in DC disclosed that PGE_2 modulated IL-23 production in a concentration and receptor usage-dependent manner that showed significant individual differences. The stimulatory effect was traced to EP4 and mimicked by an EPAC mimetic, whereas the EP2 receptor, which induced a higher elevation of the intracellular levels of cAMP, did not affect *IL23A* mRNA expression [10]. Consistent with previous reports showing that PGE_2 inhibits the expression of *IL12B* mRNA in response to stimuli such as LPS and CD40L, zymosan can be added to the list of those stimuli, although the extent of inhibition was lower than that observed in response to LPS. Unlike COX-1 inhibition, the selective COX-2 inhibitor sc-236 significantly

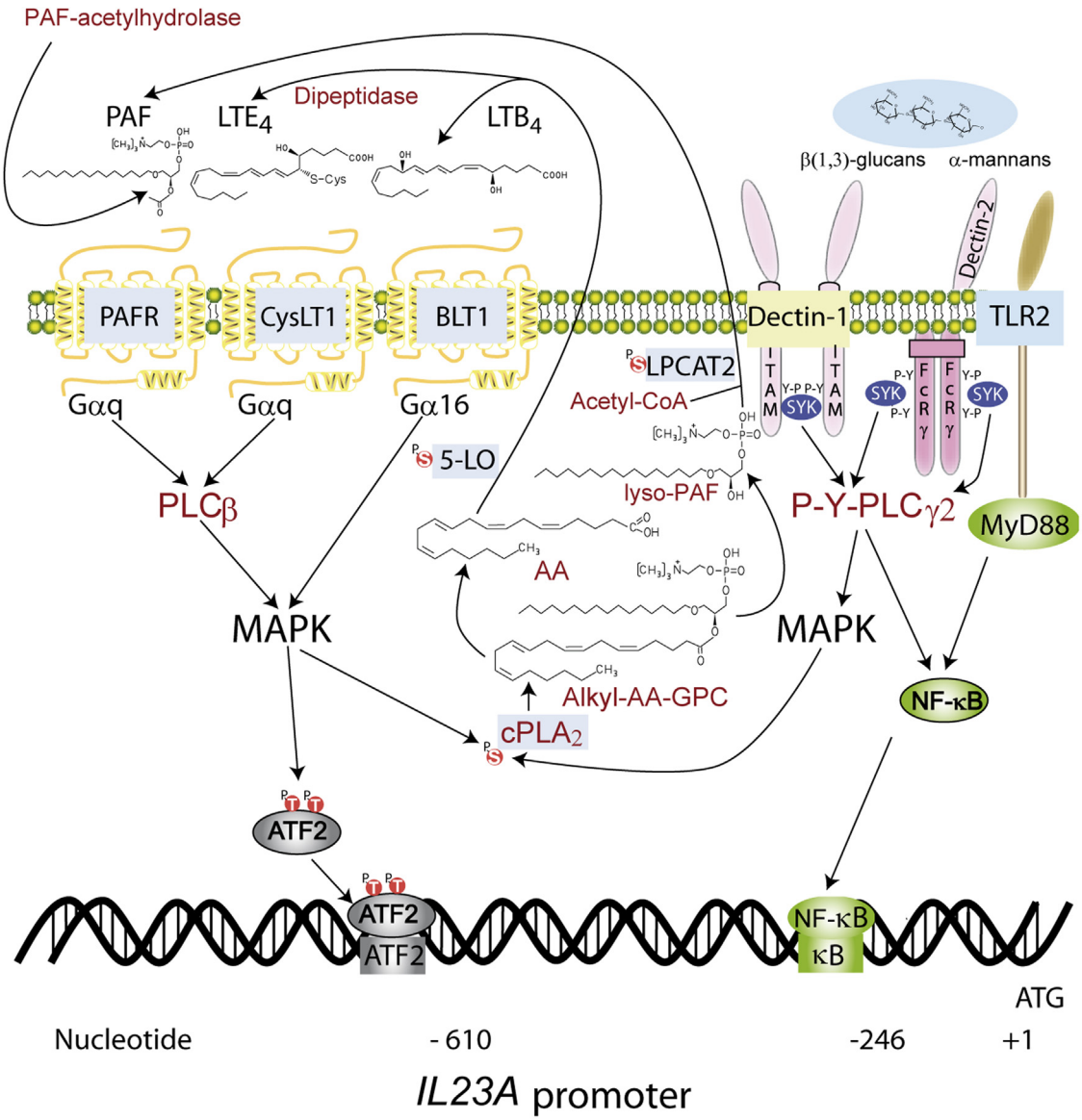

Fig. 11. Autocrine lipid mediators cooperate with fungal patterns to induce ATF2 phosphorylation and the *trans*-activation of *IL23A*. Binding of fungal patterns activates the proteins of the NF-κB family and a phosphorylation cascade involving at least PKC and MAPK that phosphorylates ATF2 at Thr69 and Thr71, $cPLA_2$ at Ser505, 5-LO at Ser663, and LPCAT at Ser34. P-Ser505-$cPLA_2$ hydrolyses 1-alkyl-2-arachidonoyl-*sn*-glycero-3-phosphocholine (Alkyl-AA-GPC) and generates both free AA and 1-alkyl-2-lyso-glycero-3-phosphocholine (lyso-PAF) that by the action of 5-LO and LPCAT1/2 give rise to LTB_4, cysteinyl-LT, and PAF. The preferential detection of LTE_4 and the increased concentrations of PAF upon darapladib treatment can be explained by the presence of dipeptidase and PAF-acetylhydrolase activities. The lipid mediators activate another signaling cascade that further enhances their biosynthesis and the phosphorylation of ATF2. The combined action of NF-κB and ATF2 on the *IL23A* promoter allows its *trans*-activation. FcRγ, Fc receptor γ-chain; ITAM, immunoreceptor tyrosine-based activation motif; PLCβ, phospholipase Cβ; PLCγ2, phospholipase Cγ2; P, phosphate; P-Y, phosphotyrosine; SYK, spleen tyrosine kinase; TLR2, Toll-like receptor 2.

decreased *IL12B* mRNA expression. Again, this can be explained on the basis of the different affinities and desensitization rates of the different EP receptors, since they may activate CREB and C/EBPβ by promoting their phosphorylation or in the case of EP2 repressing C/EBPβ through the activation of CCAAT displacement protein [61]. Given that COX-2 produces a sustained and delayed production of PGE_2 coincidental with the formation of secondary mediators, for instance TNFα and IL-6, and PGE_2 is a selective inducer of IL-12 p40 in the presence of TNFα, cooperation of these mediators seems likely. The prominent inhibition of *IL12B* elicited by sc-236 on the response to LPS is consistent with this notion, although an off-target effect can not be ruled out.

AA and PAF metabolism are closely related because 1-alkyl-phosphatidylcholine represents approximately half of the phospholipid content of myeloid cells and it is enriched in AA [62]. In keeping with these results, PAF production and PAF-induced *in vitro* directional migration of DC have been reported [35]. LPCAT enzymes participate in phospholipid remodeling in the Lands' cycle and show distinct catalytic properties and tissue distribution. LPCAT3 plays a key role in triglyceride secretion and is expressed at high levels in hepatocytes and intestinal cells [63–65], whereas these cell express very low levels of LPCAT1 and LPCAT2. Conversely, DC express both LPCAT1 and LPCAT2. LPCAT1 can use either palmitoyl-CoA or acetyl-CoA to produce dipalmitoylphosphatidylcholine and PAF, respectively. Its activity in type II pneumocytes is central in the fetal-to-maternal signaling that initiates parturition [66]. LPCAT2 can use AA-CoA and acetyl-CoA and its high expression in myeloid cells allows PAF biosynthesis.

The functional relevance of LPCAT1/2 was supported by the efficient formation of PAF C16:0 in the cell-free system and in the conditioned media. The predominance of PAF C16:0 agrees with remodeling through LPCAT1, because this enzyme shows a high activity for the biosynthesis of C16:0 species, and with the detectable production of PAF C16:0 observed in the presence of darapladib [67]. This finding and the presence of unesterified AA in resting cells suggest that PAF production might be the result of a continuous synthesis by LPCAT activities in the Lands' cycle involving phospholipase activity, acetylation of lyso-PAF by LPCAT, hydrolysis of PAF by PAF-acetylhydrolase, and new synthesis of 1-hexadecyl-2-arachidonoyl-*sn*-glycero-3-phosphorylcholine by LPCAT activity during membrane remodeling [68]. This cycle may be fine-tuned by pro-inflammatory stimuli because MAP kinases and Ca^{2+}-signaling regulate both $cPLA_2$ [69] and LPCAT2 [30,31]. Notably, a recent study has reported that this cycle may be subverted by phosphorylcholine-bearing microbes through molecular mimicry mechanisms, since these bacteria contain a phosphorylcholine-remodeling enzyme that cleaves PAF. In an experimental model of infection with *Streptococcus pneumoniae*, the absence of PAF function decreased host defense, thus suggesting that targeting PAF-acetylhydrolase could be a helpful mechanism to overcome bacterial immune evasion [70]. Given the strong ability of DC to carry out non-opsonic phagocytosis of zymosan [71], as compared to the predominant opsonic phagocytosis in polymorphonuclears [42], our data put forward a scenario involving pattern recognition receptors and lipid mediators that generates a milieu suitable for the induction of the Th17 immune response. The high concentration of free AA detected can be explained by the efficient hydrolysis by $cPLA_2$ and the catalytic properties of LPCAT2. LPCAT2 shows a significant increase of the V_{max} and a reduction of its K_m value for acetyl-CoA after Ser34 phosphorylation, whereas the K_m value for AA-CoA is increased, thus suggesting a preferential formation of PAF versus 1-alkyl-2-arachidonoyl-*sn*-glycero-3-phosphocholine under these conditions. The direct usage of AA by LPCAT can be limited by the requirement for a two-step reaction catalyzed by acyl-CoA synthetase that consumes ATP. In addition, the robust formation of 12-HETE, 15-HETE, and AA from AA-CoA in the cell-free system suggests competition by acyl-CoA thioesterases as an alternative route to the usage by LPCAT.

The finding of glycolytic reprogramming following dectin-1 signaling has highlighted the role of the acetyl-CoA formed from citrate exported from the tricarboxylic acid cycle for DC function, including the development of trained immunity [34,72]. Citrate is exported from the mitochondria into the cytosol via the citrate shuttle SLC25A1 [73] and subsequently converted into acetyl-CoA by ATP citrate lyase, an enzyme inducible by inflammatory stimuli and a major producer of cytosolic acetyl-CoA [74]. Acetyl-CoA can be channelled to the production of malonyl-CoA by acetyl-CoA carboxylase and elongation of fatty acid chains, used in lysine acetylation reactions, and as shown in this study, utilized by LPCAT enzymes. These routes may explain the changes in the level of cytosolic acetyl-CoA, which include a significant drop at one hour, consistent with the time course of phagocytosis, and a late increase, most likely explained by the glycolytic burst.

Together, our results show that fungal patterns trigger a strong release of AA and a partial conversion into its oxidative metabolism products, which include PGE_2, 12-HETE, LTB_4, and cysteinyl-LT. The generation of lyso-PAF and acetyl-CoA, together with the catalytic properties of LPCAT1/2 explain the coincidental formation of the phospholipid PAF. The combined action of LTB_4, cysteinyl-LT, and PAF on their receptors triggers a signaling cascade that contributes to the phosphorylation of ATF2 and *IL23A* promoter *trans*-activation (Fig. 11). These data provide mechanistic clues to modulate the immune response by acting on the lipid mediator cascade in diseases in which IL-23 and the Th17 immune response are involved, for instance, fungal invasive infection, psoriatic arthritis, ankylosing spondylitis, multiple sclerosis, and Crohn's disease.

Conflict of interest

The authors have declared that they have no conflict of interest.

Author's contribution

MR, SM, and SA conducted experiments. OM carried out UPLC/MS assays. JGF, MSC, and NF designed research studies and wrote the manuscript.

Acknowledgments

Dr. Jesús Pla from Universidad Complutense de Madrid, Spain, is thanked for providing *Candida albicans*. Staff from Centro de Hemoterapia y Hemodonación de Castilla y León is thanked for help with blood cell purification. This work was supported by grants from Plan Nacional de Salud y Farmacia (grant SAF2013-44521-R to MSC), Fundación Ramón Areces, Red Temática de Investigación Cardiovascular, and Gerencia Regional de Salud de Castilla y León (grant GRS 920-A-14 to JGF).

References

[1] K.M. Dennehy, J.A. Willment, D.L. Williams, G.D. Brown, Reciprocal regulation of IL-23 and IL-12 following co-activation of Dectin-1 and TLR signaling pathways, Eur. J. Immunol. 39 (2009) 1379–1386.
[2] H. Huang, G.R. Ostroff, C.K. Lee, J.P. Wang, C.A. Specht, S.M. Levitz, Distinct patterns of dendritic cell cytokine release stimulated by fungal β-glucans and toll-like receptor agonists, Infect. Immun. 77 (2009) 1774–1781.
[3] Y. Alvarez, C. Municio, E. Hugo, J. Zhu, S. Alonso, X. Hu, et al., Notch- and transducin-like enhancer of split (TLE)-dependent histone deacetylation explain interleukin 12 (IL-12) p70 inhibition by zymosan, J. Biol. Chem. 286 (2011) 16583–16595.
[4] Y. Alvarez, M. Rodríguez, C. Municio, E. Hugo, S. Alonso, N. Ibarrola, et al., Sirtuin 1 is a key regulator of the IL-12 p70/IL-23 balance in human dendritic cells, J. Biol. Chem. 287 (2012) 35689–35701.
[5] F. Al-Salleeh, T.M. Petro, Promoter analysis reveals critical roles for SMAD-3 and ATF-2 in expression of IL-23 p19 in macrophages, J. Immunol. 181 (2008) 4523–4533.
[6] O. Brain, B.M. Owens, T. Pichulik, P. Allan, E. Khatamzas, A. Leslie, et al., The intracellular sensor NOD2 induces microRNA-29 expression in human dendritic cells to limit IL-23 release, Immunity 39 (2013) 521–536.
[7] M. Rodríguez, E. Domingo, S. Alonso, J.G. Frade, J. Eiros, M. Sánchez Crespo, et al., The unfolded protein response and the phosphorylations of activating transcription factor 2 in the trans-activation of *IL23A* produced by β-glucans, J. Biol. Chem. 289 (2014) 22942–22957.
[8] S.P. Smeekens, F.L. van de Veerdonk, J.W. van der Meer, B.J. Kullberg, L.A. Joosten, M.G. Netea, The *Candida* Th17 response is dependent on mannan- and β-glucan-induced prostaglandin E_2, Int. Immunol. 22 (2010) 889–895.
[9] V.P. Kocieda, S. Adhikary, F. Emig, Y.H. Yen, M.G. Toscano, D. Ganea, Prostaglandin E_2-induced IL-23 p19 subunit is regulated by cAMP-responsive element-binding protein and C/AATT enhancer-binding protein β in bone marrow-derived dendritic cells, J. Biol. Chem. 287 (2012) 36922–36935.
[10] N.J. Poloso, P. Urquhart, A. Nicolaou, J. Wang, D.F. Woodward, PGE_2 differentially regulates monocyte-derived dendritic cell cytokine responses depending on receptor usage (EP2/EP4), Mol. Immunol. 54 (2013) 284–295.
[11] K.W. Kalim, M. Groettrup, Prostaglandin E_2 inhibits IL-23 and IL-12 production by human monocytes through down-regulation of their common p40 subunit, Mol. Immunol. 53 (2013) 274–282.
[12] S. Suram, G.D. Brown, M. Ghosh, S. Gordon, R. Loper, P.R. Taylor, et al., Regulation of cytosolic phospholipase A_2 activation and cyclooxygenase 2 expression in macrophages by the β-glucan receptor, J. Biol. Chem. 281 (2006) 5506–5514.
[13] I. Valera, N. Fernández, A.G. Trinidad, S. Alonso, G.D. Brown, A. Alonso, et al., Costimulation of dectin-1 and DC-SIGN triggers the arachidonic acid cascade in human monocyte-derived dendritic cells, J. Immunol. 180 (2008) 5727–5736.
[14] R. Parti, R. Loper, G.D. Brown, S. Gordon, P.R. Taylor, J.V. Bonventre, et al., Cytosolic phospholipase A_2 activation by *Candida albicans* in alveolar macrophages: role of dectin-1, Am. J. Respir. Cell Mol. Biol. 42 (2010) 415–423.
[15] M. Rodríguez, E. Domingo, C. Municio, Y. Alvarez, E. Hugo, N. Fernández, et al., Polarization of the innate immune response by prostaglandin E_2: a puzzle of receptors and signals, Mol. Pharmacol. 85 (2014) 187–197.

[16] S. Suram, L.J. Silveira, S. Mahaffey, G.D. Brown, J.V. Bonventre, D.L. Williams, et al., Cytosolic phospholipase $A_2\alpha$ and eicosanoids regulate expression of genes in macrophages involved in host defense and inflammation, PLoS One 8 (7) (2013) e69002.

[17] J. Song, X. Liu, T.S. Rao, L. Chang, M.J. Meehan, J.M. Blevitt, et al., Phenotyping drug polypharmacology via eicosanoid profiling of blood, J. Lipid Res. 56 (2015) 1492–1500.

[18] Y. Alvarez, C. Municio, S. Alonso, M. Sánchez Crespo, N. Fernández, The induction of IL-10 by zymosan in dendritic cells depends on CREB activation by the coactivators CREB-binding protein and TORC2 and autocrine PGE_2, J. Immunol. 183 (2009) 1471–1479.

[19] I. Morgunov, P.A. Srere, Interaction between citrate synthase and malate dehydrogenase: substrate channeling of oxaloacetate, J. Biol. Chem. 273 (1998) 29540–29544.

[20] S.E. Elcombe, S. Naqvi, M.W. Van Den Bosch, K.F. MacKenzie, F. Cianfanelli, G.D. Brown, et al., Dectin-1 regulates IL-10 production via a MSK1/2 and CREB dependent pathway and promotes the induction of regulatory macrophage markers, PLoS One 8 (3) (2013) e60086.

[21] F. Alonso, M.G. Gil, M. Sánchez-Crespo, J.M. Mato, Activation of 1-alkyl-2-lysoglycero-3-phosphocholine: acetyl-CoA transferase during phagocytosis in human polymorphonuclear leukocytes, J. Biol. Chem. 257 (1982) 3376–3378.

[22] H. Shindou, D. Hishikawa, H. Nakanishi, T. Harayama, S. Ishii, R. Taguchi, A single enzyme catalyzes both platelet-activating factor production and membrane biogenesis of inflammatory cells. Cloning and characterization of acetyl-CoA:lyso-PAF acetyltransferase, J. Biol. Chem. 282 (2007) 6532–6539.

[23] C.H. Serezani, S. Kane, L. Collins, M. Morato-Marques, J.J. Osterholzer, M. Peters-Golden, Macrophage dectin-1 expression is controlled by leukotriene B_4 via a GM-CSF/PU.1 axis, J. Immunol. 189 (2012) 906–915.

[24] K.R. Lynch, G.P. O'Neill, Q. Liu, D.S. Im, N. Sawyer, K.M. Metters, et al., Characterization of the human cysteinyl leukotriene CysLT1 receptor, Nature 399 (1999) 789–793.

[25] N. Uozumi, K. Kume, T. Nagase, N. Nakatani, S. Ishii, F. Tashiro, et al., Role of cytosolic phospholipase A_2 in allergic response and parturition, Nature 390 (1997) 618–622.

[26] M.M. Koga, B. Bizzarro, A. Sá-Nunes, F.J.O. Rios, S. Jancar, Activation of PAF-receptor induces regulatory dendritic cells through PGE_2 and IL-10, Prostaglandins Leukot. Essent. Fatty Acids 89 (2013) 319–326.

[27] C. Platzer, E. Fritsch, T. Elsner, M.H. Lehmann, H.D. Volk, S. Prösch, Cyclic adenosine monophosphate-responsive elements are involved in the transcriptional activation of the human IL-10 gene in monocytic cells, Eur. J. Immunol. 29 (1999) 3098–3104.

[28] K. Clark, K.F. MacKenzie, K. Petkevicius, Y. Kristariyanto, J. Zhang, H.G. Choi, et al., Phosphorylation of CRTC3 by the salt-inducible kinases controls the interconversion of classically activated and regulatory macrophages, Proc. Natl. Acad. Sci. U. S. A. 109 (2012) 16986–16991.

[29] P. Kalinski, P.L. Vieira, J.H. Schuitemaker, E.C. de Jong, M.L. Kapsenberg, Prostaglandin E_2 is a selective inducer of interleukin-12 p40 (IL-12p40) production and an inhibitor of bioactive IL-12p70 heterodimer, Blood 97 (2001) 3466–3469.

[30] R. Morimoto, H. Shindou, M. Tarui, T. Shimizu, Rapid production of platelet-activating factor is induced by protein kinase Cα-mediated phosphorylation of lysophosphatidylcholine acyltransferase 2 protein, J. Biol. Chem. 289 (2014) 15566–15576.

[31] R. Morimoto, H. Shindou, Y. Oda, T. Shimizu, Phosphorylation of lysophosphatidylcholine acyltransferase 2 at Ser34 enhances platelet-activating factor production in endotoxin-stimulated macrophages, J. Biol. Chem. 285 (2010) 29857–29862.

[32] S.M. Prescott, G.A. Zimmerman, D.M. Stafforini, T.M. McIntyre, Platelet-activating factor and related lipid mediators, Annu. Rev. Biochem. 69 (2000) 419–445.

[33] H. Shindou, T. Shimizu, Acyl-CoA:lysophospholipid acyltransferases, J. Biol. Chem. 284 (2009) 1–5.

[34] B. Everts, E. Amiel, S.C. Huang, A.M. Smith, C.H. Chang, W.Y. Lam, et al., TLR-driven early glycolytic reprogramming via the kinases TBK1-IKKε supports the anabolic demands of dendritic cell activation, Nat. Immunol. 15 (2014) 323–332.

[35] S. Sozzani, D. Longoni, R. Bonecchi, W. Luini, L. Bersani, G. D'Amico, et al., Human monocyte-derived and $CD34^+$ cell-derived dendritic cells express functional receptors for platelet activating factor, FEBS Lett. 418 (1997) 98–100.

[36] O.M. Pello, M. De Pizzol, M. Mirolo, L. Soucek, L. Zammataro, A. Amabile, et al., Role of c-MYC in alternative activation of human macrophages and tumor-associated macrophage biology, Blood 119 (2012) 411–421.

[37] T. Rothe, F. Gruber, S. Uderhardt, N. Ipseiz, S. Rössner, O. Oskolkova, et al., 12/15-Lipoxygenase-mediated enzymatic lipid oxidation regulates DC maturation and function, J. Clin. Invest. 125 (2015) 1944–1954.

[38] K.H. Brettingham-Moore, S. Rao, T. Juelich, S. Frances, M.F. Shannon, A.F. Holloway, GM-CSF promoter chromatin remodelling and gene transcription display distinct signal and transcription factor requirements, Nucl. Acids Res. 33 (2005) 225–234.

[39] M. Nakamura, T. Shimizu, Leukotriene receptors, Chem. Rev. 111 (2011) 6231–6298.

[40] S. Markoutsa, D. Sürün, M. Karas, B. Hofmann, D. Steinhilber, B.L. Sorg, Analysis of 5-lipoxygenase phosphorylation on molecular level by MALDI-MS, FEBS J. 281 (2014) 1931–1947.

[41] R.A. Lepley, D.T. Muskardin, F.A. Fitzpatrick, Tyrosine kinase activity modulates catalysis and translocation of cellular 5-lipoxygenase, J. Biol. Chem. 271 (1996) 6179–6184.

[42] B.B. Rubin, G.P. Downey, A. Koh, N. Degousee, F. Ghomashchi, L. Nallan, et al., Cytosolic phospholipase $A_2\alpha$ is necessary for platelet-activating factor biosynthesis, efficient neutrophil-mediated bacterial killing, and the innate immune response to pulmonary infection: $cPLA_2\alpha$ does not regulate neutrophil NADPH oxidase activity, J. Biol. Chem. 280 (2005) 7519–7529.

[43] M.W. Buczynski, D.L. Stephens, R.C. Bowers-Gentry, A. Grkovich, R.A. Deems, E. A. Dennis, TLR-4 and sustained calcium agonists synergistically produce eicosanoids independent of protein synthesis in RAW264.7 cells, J. Biol. Chem. 282 (2007) 22834–22847.

[44] M. Pinot, S. Vanni, S. Pagnotta, S. Lacas-Gervais, L.A. Payet, T. Ferreira, Polyunsaturated phospholipids facilitate membrane deformation and fission by endocytic proteins, Science 345 (2014) 693–697.

[45] I. Szatmari, D. Töröcsik, M. Agostini, T. Nagy, M. Gurnell, E. Barta, et al., PPARγ regulates the function of human dendritic cells primarily by altering lipid metabolism, Blood 110 (2007) 3271–3280.

[46] M. Luo, S.M. Jones, M.J. Coffey, M. Peters-Golden, T.G. Brock, Protein kinase A inhibits leukotriene synthesis by phosphorylation of 5-lipoxygenase on serine 523, J. Biol. Chem. 279 (2004) 41512–41520.

[47] M. Luo, S.M. Jones, N. Flamand, D.M. Aronoff, M. Peters-Golden, T.G. Brock, Phosphorylation by protein kinase A inhibits nuclear import of 5-lipoxygenase, J. Biol. Chem. 280 (2005) 40609–40616.

[48] O. Werz, D. Szellas, D. Steinhilber, O. Rådmark, Arachidonic acid promotes phosphorylation of 5-lipoxygenase at Ser-271 by MAPK-activated protein kinase 2 (MK2), J. Biol. Chem. 277 (2002) 14793–14800.

[49] J. Esser, U. Gehrmann, M.D. Salvado, A. Wetterholm, J.Z. Haeggström, B. Samuelsson, et al., Zymosan suppresses leukotriene C_4 synthase activity in differentiating monocytes: antagonism by aspirin and protein kinase inhibitors, FASEB J. 25 (2011) 1417–1427.

[50] P.C. Norris, D. Gosselin, D. Reichart, C.K. Glass, E.A. Dennis, Phospholipase A_2 regulates eicosanoid class switching during inflammasome activation, Proc. Natl. Acad. Sci. U. S. A. 111 (2014) 12746–12751.

[51] R. Gaudreau, C. Le Gouill, S. Métaoui, S. Lemire, J. Stankovà, M. Rola-Pleszczynski, Signalling through the leukotriene B_4 receptor involves both α_i and α_{16}, but not α_q or α_{11} G-protein subunits, Biochem. J. 335 (1998) 15–18.

[52] C.K. Weber, J.R. Slupsky, H.A. Kalmes, U.R. Rapp, Active Ras induces heterodimerization of cRaf and BRaf, Cancer Res. 61 (2001) 3595–3598.

[53] A.M. Liu, R.K. Lo, M.M. Lee, Y. Wang, W.W. Yeung, M.K. Ho, et al., $G\alpha_{16}$ activates Ras by forming a complex with tetratricopeptide repeat 1 (TPR1) and Son of Sevenless (SOS), Cell Signal. 22 (2010) 1448–1458.

[54] S.L. Brown, V.R. Jala, S.K. Raghuwanshi, M.W. Nasser, B. Haribabu, R.M. Richardson, Activation and regulation of platelet-activating factor receptor: role of G_i and G_q in receptor-mediated chemotactic, cytotoxic, and cross-regulatory signals, J. Immunol. 177 (2006) 3242–3249.

[55] M. Hoshino, T. Izumi, T. Shimizu, Leukotriene D_4 activates mitogen-activated protein kinase through a protein kinase Cα-Raf-1-dependent pathway in human monocytic leukemia THP-1 cells, J. Biol. Chem. 273 (1999) 4878–4882.

[56] H.M. Sarau, R.S. Ames, J. Chambers, C. Ellis, N. Elshourbagy, J.J. Foley, et al., Identification, molecular cloning, expression and characterization of a cysteinyl leukotriene receptor, Mol. Pharmacol. 56 (2009) 657–663.

[57] O. Sözeri, K. Vollmer, M. Liyanage, D. Frith, G. Kour, G.E. Mark 3rd, S. Stabel, Activation of the c-Raf protein kinase by protein kinase C phosphorylation, Oncogene 7 (1992) 2259–2262.

[58] W. Kolch, G. Heidecker, G. Kochs, R. Hummel, H. Vahidi, H. Mischak, et al., Protein kinase C alpha activates RAF-1 by direct phosphorylation, Nature 364 (1993) 249–252.

[59] N.N. Huang, S. Becker, C. Boularan, O. Kamenyeva, A. Vural, I.Y. Hwang, et al., Canonical and noncanonical G-protein signaling helps coordinate actin dynamics to promote macrophage phagocytosis of zymosan, Mol. Cell. Biol. 34 (2014) 4186–4199.

[60] T. Khayrullina, J.H. Yen, H. Ping, D. Ganea, In vitro differentiation of dendritic cells in the presence of prostaglandin E_2 alters the IL-12/IL-23 balance and promotes differentiation of Th17 cells, J. Immunol. 181 (2008) 721–735.

[61] H. Jing, J.H. Yen, D. Ganea, A novel signaling pathway mediates the inhibition of CCL3/4 expression by prostaglandin E_2, J. Biol. Chem. 279 (2004) 55176–55186.

[62] A. Yamashita, T. Sugiura, K. Waku, Acyltransferases and transacylases involved in fatty acid remodeling of phospholipids and metabolism of bioactive lipids in mammalian cells, J. Biochem. 122 (1997) 1–16.

[63] X. Rong, C.J. Albert, C. Hong, M.A. Duerr, B.T. Chamberlain, E.J. Tarling, et al., LXRs regulate ER stress and inflammation through dynamic modulation of membrane phospholipid composition, Cell Metab. 18 (2013) 685–697.

[64] X. Rong, B. Wang, M.M. Dunham, P.N. Hedde, J.S. Wong, E. Gratton, et al., LPCAT3-dependent production of arachidonoyl phospholipids is a key determinant of triglyceride secretion, eLIFE (2015) , doi:http://dx.doi.org/10.7554/elife.06557.

[65] T. Hashidate-Yoshida, T. Harayama, D. Hishikawa, R. Morimoto, F. Hamano, S.M. Tokuoka, et al., Fatty acyl-chain remodeling by LPCAT3 enriches arachidonate in phospholipid membranes and regulates triglyceride transport, eLIFE (2015) , doi:http://dx.doi.org/10.7554/eLife.06328.

[66] L. Gao, E.H. Rabbitt, J.C. Condon, N.E. Renthal, J.M. Johnston, M.A. Mitsche, et al., Steroid receptor coactivators 1 and 2 mediate fetal-to-maternal signaling that initiates parturition, J. Clin. Invest. 125 (2015) 2808–2824.

[67] R.S. Rosenson, D.M. Stafforini, Modulation of oxidative stress, inflammation, and atherosclerosis by lipoprotein-associated phospholipase A_2, J. Lipid Res. 53 (2012) 1767–1782.
[68] J. Chen, L. Yang, J.M. Foulks, A.S. Weyrich, G.K. Marathe, T.M. McIntyre, Intracellular PAF catabolism by PAF acetylhydrolase counteracts continual PAF synthesis, J. Lipid Res. 48 (2007) 2365–2376.
[69] L.L. Lin, M. Wartmann, A.Y. Lin, J.L. Knopf, A. Seth, R.J. Davis, $cPLA_2$ is phosphorylated and activated by MAP kinase, Cell 72 (1993) 269–278.
[70] C.B. Hergott, A.M. Roche, N.A. Naidu, C. Mesaros, I.A. Blair, J.N. Weiser, Bacterial exploitation of phosphorylcholine mimicry suppresses inflammation to promote airway infection, J. Clin. Invest. 125 (2015) 3878–3890.
[71] C. Municio, Y. Alvarez, O. Montero, E. Hugo, M. Rodríguez, E. Domingo, et al., The response of human macrophages to β-glucans depends on the inflammatory milieu, PLoS One 8 (4) (2013) e62016.
[72] S.C. Cheng, J. Quintin, R.A. Cramer, K.M. Shepardson, S. Saeed, V. Kumar, et al., mTOR- and HIF-1α-mediated aerobic glycolysis as metabolic basis for trained immunity, Science 345 (6204) (2014) , doi:http://dx.doi.org/10.1126/science.1250684.
[73] F. Palmieri, The mitochondrial transporter family (SLC25): physiological and pathological implications, Pflugers Arch. 447 (2004) 689–709.
[74] V. Infantino, V. Iacobazzi, F. Palmieri, A. Menga, ATP-citrate lyase is essential for macrophage inflammatory response, Biochem. Biophys. Res. Commun. 440 (2013) 105–111.